



# Volatile organic compounds in a typical petrochemical industrialized valley city of northwest China based on high-resolution PTR-MS measurements: Characterization, sources and chemical effects

Xi Zhou <sup>a,b</sup>, Zhongqin Li <sup>b,c,\*</sup>, Tinjun Zhang <sup>a,d</sup>, Fanglin Wang <sup>a</sup>, Feiteng Wang <sup>b</sup>, Yan Tao <sup>a</sup>, Xin Zhang <sup>c</sup>, Fanglong Wang <sup>c</sup>, Ju Huang <sup>a</sup>

<sup>a</sup> Key Laboratory of Western China's Environmental Systems (Ministry of Education), College of Earth and Environmental Sciences, Lanzhou University, Lanzhou 730000, China

<sup>b</sup> State Key Laboratory of Cryospheric Sciences, Northwest Institute of Eco-Environment and Resources, Tianshan Glaciological Station, Chinese Academy of Sciences, Lanzhou 730000, China

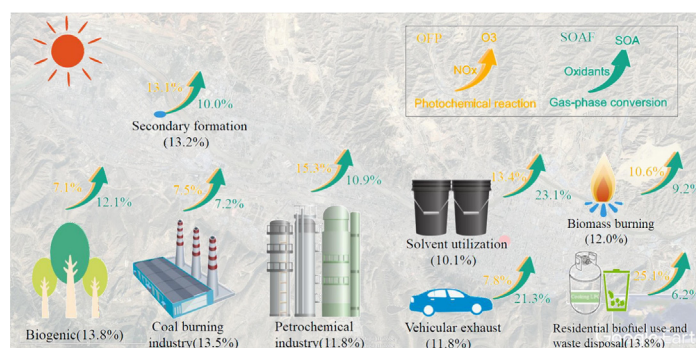
<sup>c</sup> College of Geography and Environmental Science, Northwest Normal University, Lanzhou 730000, China

<sup>d</sup> University Corporation for Polar Research, Beijing 100875, China

## HIGHLIGHTS

- Higher OVOCs were observed by PTR-MS in the Lanzhou valley.
- PMF, CPF and TSM model showed that 8-source factors and their source areas.
- Anthropogenic source accounted for 74%, and around 70% VOCs pollution was the local emission.
- O<sub>3</sub>/SOA formation potential of individual VOC and PMF-derived source factors were performed.

## GRAPHICAL ABSTRACT



## ARTICLE INFO

### Article history:

Received 7 December 2018

Received in revised form 16 March 2019

Accepted 19 March 2019

Available online 22 March 2019

Editor: Jianmin Chen

### Keywords:

PTR-MS

VOCs

Lanzhou

Source apportionment

OPF

SOAF

## ABSTRACT

To scientifically understand the emissions and chemistry of volatile organic compounds (VOCs) in a typical petrochemical industrialized and dust-rich region of Northwest China, VOCs were measured at a receptor site in the Lanzhou Valley using a high-resolution online proton transfer reaction-mass spectrometer (PTR-MS). The ranking of VOC mixing ratios was methanol ( $32.72 \pm 8.94$  ppb) > acetaldehyde ( $5.05 \pm 2.4$  ppb) > acetic acid ( $3.42 \pm 1.71$  ppb). Lanzhou has higher oxygenated VOCs (OVOCs) mixing ratios (methanol and acetaldehyde) and lower aromatics levels (benzene, toluene and C8-aromatics) compared with other cities.

The positive matrix factorization (PMF) model showed eight sources of VOCs as follows: (1) mixed industrial process-1 (13.5%), (2) secondary formation (13.2%), (3) mixed industrial process-2 (11.8%), (4) residential biofuel use and waste disposal (13.80%), (5) solvent usage (10.1%), (6) vehicular exhaust (11.8%), (7) biogenic (13.8%) and (8) biomass burning (12.0%). Both the PSCF and the CWT results of mixed industrial process-1 were mainly from the northeast of Lanzhou and the biomass burning was from the southeast; the other four sources (without secondary formation and biogenic) were mainly from the west and northwest of Lanzhou, which were associated with the dust area of the Gobi Desert. A trajectory sector analysis revealed that the local emissions contributed 64.9–71.1% to the VOCs.

\* Corresponding author at: State Key Laboratory of Cryospheric Sciences, Northwest Institute of Eco-Environment and Resources, Tianshan Glaciological Station, Chinese Academy of Sciences, Lanzhou 730000, China.

E-mail address: [lizq@lzb.ac.cn](mailto:lizq@lzb.ac.cn) (Z. Li).

OVOCs accounted for 43% of the ozone production potential (OPP), and residential biofuel use and waste disposal (25.1%), mixed industrial process-2 (15.3%) and solvent usage (13.4%) appeared to be the dominant sources contributors to O<sub>3</sub> production. The rank of main secondary organic aerosols (SOA) precursors under low-NO<sub>x</sub> conditions is xylene > toluene > benzene > naphthalene > styrene > C10-aromatics > isoprene, while under high-NO<sub>x</sub> conditions, it is toluene > naphthalene > xylene > C10-aromatics > styrene > benzene > isoprene. Solvent usage and vehicular exhaust appeared to be the dominant contributors to SOA formation.

© 2019 Elsevier B.V. All rights reserved.

## 1. Introduction

Volatile organic compounds (VOCs) have a significant influence on air quality due to their reactions by gas phase photochemistry, resulting in the formation of secondary pollutants such as tropospheric ozone (O<sub>3</sub>) and secondary organic aerosols (SOA) (Carter and Atkinson, 1989; Seinfeld and Pandis, 1998). Both O<sub>3</sub> and SOA play important roles in air quality and climate because of their effects on air quality and atmospheric radiative forcing (Lewis et al., 2000; IPCC, 2013). The VOCs' atmospheric lifetimes were in the range of several hours to tens of days (Atkinson, 2000; Jordan et al., 2009), and inhalation of certain VOCs directly affects human health. For instance, benzene and formaldehyde are considered human carcinogens (WHO, 2010). Studies involving ambient VOCs such as emissions sources, transformation processes and health impacts are relatively rare even though their influences on air pollution can be comparable to particulate matter (PM) (Huang et al., 2014).

Lanzhou city is the capital of Gansu province in Northwest China with a population of 3.2 million. It is a narrow valley city located in the downwind regions of Taklimakan and Gobi Deserts in Northwest China, affected by mineral dust and is an industrial city featuring a large-scale oil refinery and petrochemical industries. The first field evidence of photochemical smog in China was in the Lanzhou Valley in the late 1970s (Tang et al., 1989), which has been widely identified as a milestone of the modern air pollution research in China. Anthropogenic and dust pollution combined with the undiffused terrain has caused the Lanzhou Valley to become one of the most heavily polluted cities both in China and even globally (WHO, 2016), and it can be taken as a typical sample for revealing the process of ambient VOCs variation, sources and their biogeochemical effects in the northwest regions of China. Previous studies concerning the observations of VOCs in China have mostly concentrated on megalopolis clusters such as the Beijing–Tianjin–Hebei (BTH) region (Yuan et al., 2010; Li et al., 2015), the Yangtze River Delta (YRD) region (Shao et al., 2016; Mo et al., 2017; Zhu et al., 2018), the Pearl River Delta (PRD) region (Zou et al., 2015; Zhang et al., 2015), and the Chengdu-Chongqing (CC) region (Li et al., 2014; Li et al., 2018). They found traffic and solvent use were the top two contributors to the atmospheric VOCs in urban regions. However, research remains lacking in the petrochemical industrialized valley areas with many coarse particles and much mineral dust in Northwest China. Furthermore, research on air pollution in the Lanzhou Valley was mainly related to sulfur dioxide (SO<sub>2</sub>), nitrogen dioxide (NO<sub>2</sub>), carbon monoxide (CO), PM<sub>2.5</sub>, PM<sub>10</sub> and O<sub>3</sub> (Chu et al., 2008a, 2008b, 2008c; Wang et al., 2016; Zhou et al., 2018), and very little information is known about VOCs' temporal variations, emission sources, interaction with PM and mineral dust, influences to air quality and health impact.

From previous studies, the measurements of VOCs were conducted in urban areas using gas chromatography with a mass spectrometer detector (GC–MS) or flame-ionization detection (GC–FID) (Blake et al., 2009). The sensitivity and chemical detail achieved with GC methods are impressive, while the drawbacks of GC techniques include the fact that they are time- and labor-intensive, which limits the number of samples that can be analyzed in practice. Additionally, preconcentration

of VOCs is needed to achieve the lowest detection limits, and the pre-treatment of sample air to remove water, ozone, and/or carbon dioxide can lead to sampling issues requiring extensive characterization (Robert et al., 2009). PTR-MS measurements identify compounds based on the molecular formula (mass-to-charge ratio) and have a high time resolution (~0.1 s) and a low limit of detection (0.3 ppbv), and the advantage of using proton transfer is that it is a soft ionization method, which mean it generally does not lead to fragmentation of the product ions (de Gouw and Warneke, 2007). The applications of PTR-MSs have greatly promoted understanding of VOC sources and their roles in air-quality issues (Yuan et al., 2017). However, deployments of PTR-MSs in urban environments are surprisingly limited, and the studies are mainly from Indian researchers, who have deployed PTR-MSs in two south Asian cities in the winter (Sinha et al., 2014; Sarkar et al., 2016). In their measurements, high concentrations of acetaldehyde, acetonitrile, and benzene were observed in Kathmandu, Nepal. In addition, the authors detected strong signals of formamide, acetamide, nitromethane, and isocyanic acid, which may pose significant human health concerns. Therefore, continuous observation of VOCs using a PTR-MS, which is the first such instrument and disposition in Northwest China, was carried out in the early spring (23 February to 10 March) of 2017 in the Lanzhou Valley. Novel insights could be acquired regarding chemical processes related to O<sub>3</sub> and SOA formation in a complex chemical environment affected by mountain meteorology and both anthropogenic and biogenic sources.

As valid statistical methods and an important prerequisite for source apportionment, receptor models have been widely used to identify VOC sources, including principal component analysis/absolute principal component scores (PCA/APCSs), chemical mass balance (CMB) and positive matrix factorization (PMF) (Debevec et al., 2017). The PMF multivariate receptor model has recently been the most used method, which can apportion VOCs levels to their emission sources by identifying substantial characteristics of the data and limiting all the elements in the factor profiles and the factor loading matrix to positive values (Yuan et al., 2009). Meanwhile, the geographic origins models including conditional probability function (CPF), potential source contribution function (PSCF) and the concentration weighted trajectory (CWT) models and a trajectory sector analysis were applied to identify the orientation of the local and regional origins derived by the PMF model. Recently, the combination of the two models has been employed to determine atmospheric pollutants origins and their locations for targeted mitigation of VOCs pollution, but it mainly concerned the ambient PM, and few studies have concentrated on the emission source contributions of VOCs (Zheng et al., 2018).

For the purpose of supplying gaps in scientific understanding regarding the characteristics and interactions of VOCs, a typical petrochemical industrialized dust valley in Northwest China was chosen as the study region to implement the observations of VOCs with high time and sensibility resolution. The objectives of this study are (1) to provide the current VOCs levels and temporal behaviors in the Lanzhou Valley and compare them with other cities, (2) to identify major pollution sources and regions of VOCs by the PMF model, the CPF model, and trajectory statistical models (TSM), and (3) to quantify the impacts of VOCs on secondary pollutants (O<sub>3</sub> and SOA).

## 2. Experiment and methods

### 2.1. Site description and additional data available

Fig. 1 shows the location of the Lanzhou Valley and the sampling site. The Lanzhou Valley is located at a narrow (2–8 km width), long (40 km), NW-SE oriented valley basin with the average elevation of ~1600 m above the sea level, which is belong to the high-altitude city. The sampling site is located in the eastern of Lanzhou urban areas and also in a distinct location where air masses are affected by various different origin regions, including the metropolitan Chengguan district, the petrochemical industrialized Xigu district and the Qilihe and Anning districts with mixed cultivation and residential areas. For the measurements of pollutant concentrations, standard methods were used based on GB3095–2012 specifications (<http://hbj.new.ccqcs.gov.cn/upfiles/2013-3/2013327153015207.pdf>) as follows: for CO—gas filter correlation infrared absorption method (TEI Model 48i from Thermo Fisher Scientific Inc., USA), and for NO<sub>2</sub>—the chemiluminescence method (TEI Model 42i from Thermo Fisher Scientific Inc., USA), and for O<sub>3</sub>—the UV-spectrophotometry method (TEI Model 49i from Thermo Fisher Scientific Inc., USA). Meteorological data such as atmospheric temperature (T), pressure (Phpa), relative humidity (RH), solar radiation (SR), wind speed (WS) and direction (WD) were obtained from Lanzhou surface meteorological station.

### 2.2. PTR-MS measurements

The PTR-MS instrument (Ionicon Analytik GmbH, Innsbruck, Austria) was used for this research. Briefly, (1) reagent ions, H<sub>3</sub>O<sup>+</sup>, were produced from a pure flow in a hollow cathode discharge ion source, (2) VOCs in the ambient air were introduced from the injection port into the drift tube where provided steady electric fields, and were ionized by proton transfer reactions:



(3) a quadrupole mass filter (QMS) and a secondary electron multiplier (SEM) allows mass separation and detection of the reagent ions (H<sub>3</sub>O<sup>+</sup>) and product ions (VOCH<sup>+</sup>) (de Gouw et al., 2003). The PTR-MS instrument was installed in a thermostatic ultra-clean room on the roof of the research building of Chinese Academy of Sciences (CAS, ~25 m above ground) during 23 February to 10 March 2017. The sample air was incessantly through a 1/16" PEEK inlet line (0.1 mm ID, ~5 m length) that was protected with a 1/8" Teflon line. An inline particulate filter was used to avoid sand dust and debris pieces entering the sampling inlet.

The technique of PTR-MS and its application for detecting VOCs in air samples at pptv level has been extensively validated in urban, rural and

forested regions of the world and has been described in two comprehensive reviews by de Gouw and Warneke (2007) and Blake et al. (2009). To guarantee the data quality acquired from PTR-MS system during this deployment in the present study, the mass spectrometer tuning, blank experiment, and instrument calibration were conducted regularly.

The PTR-MS was operated with a drift tube pressure of 2.3 mbar, a voltage of 600 V, and a temperature of 60 °C, leading to an E/N ratio of ~135 Td. VOCs were continuously observed using the instrument with a full-scan mode (from m/z 20 to 200 with one cycle of 28.5 s). Throughout the measurement period, the primary ion count (signal due to the main reagent H<sub>3</sub>O<sup>+</sup> ions) in the instrument was always above 1.5 × 10<sup>5</sup> ncps, enabling excellent detection sensitivity. Further, the impurity ion signals due to NO<sup>+</sup> and O<sub>2</sub><sup>+</sup> were always <0.7% and 3.4% of the primary ion signal, respectively. Three calibrations were performed (before, during and after the observation) by diluting dynamically VOC gas standards (TO-14A, Restek, Bellefonte, PA, USA). For measuring the background values, zero-air generated by a catalytic converter was sampled into the PTR-MS, which heated to 250 °C (GCU-0703, Ionicon Analytik GmbH, Austria) to remove chemical species. The daily mean background signal was subtracted from the VOCs observation concentration. 3 σ of the baseline value was determined as the limit of detection (LOD) of VOCs, and all were below 0.3 ppb in this work. The measurement uncertainty was estimated at ±20%, considering errors on baseline value, calibrations, RH, linearity and reproducibility, which indicated the instrument was relatively stable. Fig. S1 shows the sensitivities (ncps ppb<sup>-1</sup>) for acetonitrile (a biomass burning tracer), acetaldehyde (an oxygenated compound), isoprene (a biogenic tracer) and benzene (an aromatic compound) during the calibration experiments. For chemicals not found in the calibration gas, their respective ion count rate was directly converted into a concentration unit using transmission curve coefficients (de Gouw and Warneke, 2007; Taipale et al., 2008), by using the transmission tool of the PTR-MS Viewer software (Version 3.1.0.28, Ionicon Analytik GmbH) and calibration results. Transmission coefficients of masses not calibrated were obtained interpolating known transmission coefficients according to a cubic Hermite spline (Taipale et al., 2008). The transmission values of calibration gas were employed such as benzene (m/z = 79), toluene (m/z = 93), xylenes (m/z = 107), trimethylbenzenes (m/z = 121), dichlorobenzene (m/z = 146) and trichlorobenzene (m/z = 180).

### 2.3. PMF model

The PMF 5.0 model was performed to VOCs data observed by the PTR-MS instrument for source apportionment (USEPA, 2014; Liu et al., 2016; Mo et al., 2017). The PMF model is a multivariate factor statistical

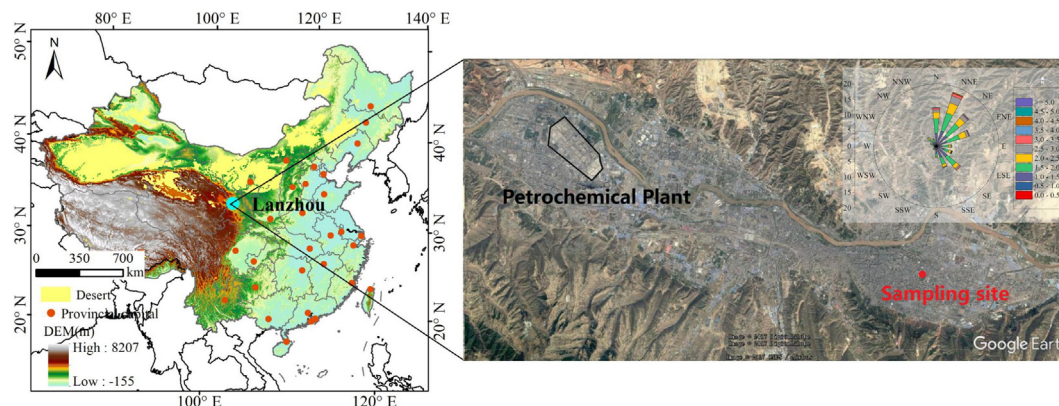


Fig. 1. Location of Lanzhou city in China (left) and the measurement site (right).

method that decomposes the observation data matrix  $x$  of  $i$  by  $j$  dimensions into two matrices: factor contributions ( $g$ ) and factor profiles ( $f$ ) (Paatero and Tapper, 1994; Paatero, 1997):

$$X_{ij} = \sum_{k=1}^{\bar{p}} g_{ik} f_{kj} + e_{ij} \quad (2)$$

The best PMF solution was minimized the objective function  $Q$  on the basis of the uncertainties (Unc)  $u_{ij}$ :

$$Q = \sum_{i=1}^n \sum_{j=1}^m \left[ \frac{x_{ij} - \sum_{k=1}^{\bar{p}} g_{ik} f_{kj}}{u_{ij}} \right]^2 \quad (3)$$

where  $\bar{p}$  is the factors' number,  $e_{ij}$  is the residual for considered samples,  $m$  is the number of each species, and  $n$  is the number of samples. To initiate the PMF 5.0 model, two input files, concentration values and uncertainty values for each species, are required. The uncertainties were calculated with the following eq. (MDL is the method detection limit):

$$U_{nc} = \begin{cases} MDL \times \frac{5}{6}, & conc. \leq MDL \\ \sqrt{MDL^2 + (\text{Error fraction} \times conc.)^2}, & conc. \geq MDL \end{cases} \quad (4)$$

We selected a suite of VOCs samples for the source apportionment analysis with less uncertainty as follows: (1) samples indicative of VOC sources (i.e., acetonitrile is the biomass burning tracer and isoprene is the biogenic tracer) are retained and (2) samples missing >25% data are excluded, and a small amount of missing data could be replaced by samples mean concentration. Eventually, 35 VOC species were selected to determine the VOCs sources, and an 8-factor solution was deemed to be the best PMF model solution, which was assessed by the  $Q/Q_{\text{theory}}$  ratio, the species residuals distributions, the plausibility of the source profiles and the constraints condition imposed by the rotational ambiguity of the solution. In this work, all the  $Q/Q_{\text{theory}}$  ratios are <1, even for the 3-factor solution with no physical interpretability; therefore, the absolute value was helpless for the optimum factors' number decision. Fig. S2 shows that the number of factors has almost no impact on how well the total mass is reproduced by the model, but when the factors' number increased to 8, the  $Q/Q_{\text{theory}}$  ratio was realized to be the last distinct drop, which is consistent with the result from Sarkar et al. (2017). The 7-factor solution was unable to distinguish the mixed industrial process-2 factor, while the 9-factor solution separated an indecipherable factor. Most of the residuals are distributed normally, ranging from  $-3$  and  $+3$ , suggesting the model fit the input data well. The rotation ambiguity was explored by varying the  $F_{\text{peak}}$  values from  $-5$  to  $+5$  (Li et al., 2017), and the results with  $F_{\text{peak}} = 0$  were selected for the lowest  $dQ$  (robust), indicating the stability of the PMF solution. The observed mass concentrations of VOCs were well resolved by the PMF ( $r^2 = 0.98$ ), as shown in Fig. S3.

#### 2.4. CPF model

To assess the influence of wind direction to local emission origins, the CPF model was carried out by using the PMF source contribution solution, coupled with the corresponding wind direction values. The probability of a specific origin contribution from a particular wind direction is calculated (Fleming et al., 2012):

$$CPF = \frac{m_{\Delta\theta}}{n_{\Delta\theta}} \quad (5)$$

where  $m_{\Delta\theta}$  is the number of mean wind vectors that exceed the threshold criteria (75th percentile) from sources contributions corresponding with the specific wind sector ( $\Delta\theta = 45^\circ$ ). While  $n_{\Delta\theta}$  is the total number

of data occurring in the same wind sector. Data for wind speed  $<0.5 \text{ m}^{-1}$  were discarded.

#### 2.5. Trajectory statistical models (TSM)

Trajectory statistical models (TSM) including trajectory cluster analysis, PSCF model, CWT model and trajectory sector analysis (Bari et al., 2003; Wang et al., 2009; Dimitriou and Kassomenos, 2015; Zheng et al., 2018), and the details were showed in the Fd. S1 in the supplement.

#### 2.6. Calculation of $O_3$ and SOA formation potential

The ozone formation potential (OFP) was calculated as follow, and detailed reaction steps and interpretation were showed in the Fd. S2 in the supplement:

$$\begin{aligned} \text{OFP} &= \text{total RH OH reactivity} \times [\text{OH}] \times n \\ &= \left( \sum k_{(\text{RH}+\text{OH})} [\text{RH}_i] \right) \times 10^6 \times 2 \end{aligned} \quad (6)$$

where  $[\text{RH}_i]$  is the observed concentration of  $\text{VOC}_i$  and  $k_{\text{RH}+\text{OH}}$  is the first-order rate coefficient for the reaction of  $\text{VOC}_i$  with OH radicals (Atkinson and Arey, 2003, Atkinson et al., 2006; <http://kinetics.nist.gov/kinetics>).

The SOA formation (SOAF) was determined by using reported SOA yield under different NOx conditions (Table S1 in the supplement) as follow (Sarkar et al., 2017):

$$\text{SOAF} = [\text{VOC}]_i \times \text{SOA yield of VOC}_i \quad (7)$$

### 3. Results and discussion

#### 3.1. Characteristics of VOCs in the Lanzhou Valley

##### 3.1.1. Concentration levels and variations

Many protonated molecules values were detected to reach  $m/z$  140, most of which are odd values, and when the  $m/z$  value is higher, the signal is lower (Fig. S4). Strong ion signals were attributed to methanol (M33), propene (M43), acetaldehyde (M45), formic acid + ethanol (M47), acetone + propanal (M59), and acetic acid (M61). Meanwhile, aromatics (M79, M93, M105, M107, M121, and M135) and oxygenated VOCs (CmHnOk, M71, M73, M75, M85, M87, M89, M95, M97, M99, M101, and M129) were observed. In addition, VOCs tracers for biomass-burning sources such as acetonitrile (M42) and for biogenic sources such as isoprene (M69) were observed. Meanwhile, mean values, standard deviations (SD) and interquartile ranges (IQRs, 25th to 75th) of the major VOCs and other pollutants are summarized (Table S2). The ranking of VOC mixing ratios was methanol ( $32.72 \pm 8.94$  ppb) > acetaldehyde ( $5.05 \pm 2.4$  ppb) > acetic acid ( $3.42 \pm 1.71$  ppb) > propene ( $2.70 \pm 1.06$  ppb) > acetone + propanal ( $2.51 \pm 1.46$  ppb) > formic acid + ethanol ( $2.32 \pm 0.69$  ppb) > toluene ( $0.72 \pm 0.52$  ppb) > sum of C8-aromatics ( $0.61 \pm 0.43$  ppb).

Fig. 2 illustrates the general trend of VOC mixing ratios (10-min time resolution) from 23 February to 10 March 2017. The orange shaded rectangles in Fig. 2 shows a dust event occurred from 22:00 28 February to 17:00 1 March with high PM values (Fig. 2b), and the back trajectories of the air masses indicated long-range transport of dust from the northwest towards the site (Fig. S5; orange trajectories). VOC mixing ratios were reduced during the dust periods, and the variation values of VOC mixing ratios were shown in Fig. 4 during dust and nondust periods. Sahu et al. (2016) indicated the mixing ratios of VOCs decrease rapidly with increasing wind speed in lower wind speed regimes but decrease slowly in higher wind speed regimes in an urban site of Ahmedabad, India. In this measurement, mean wind speed reached 1.93 m/s during the dust periods with major wind direction from the

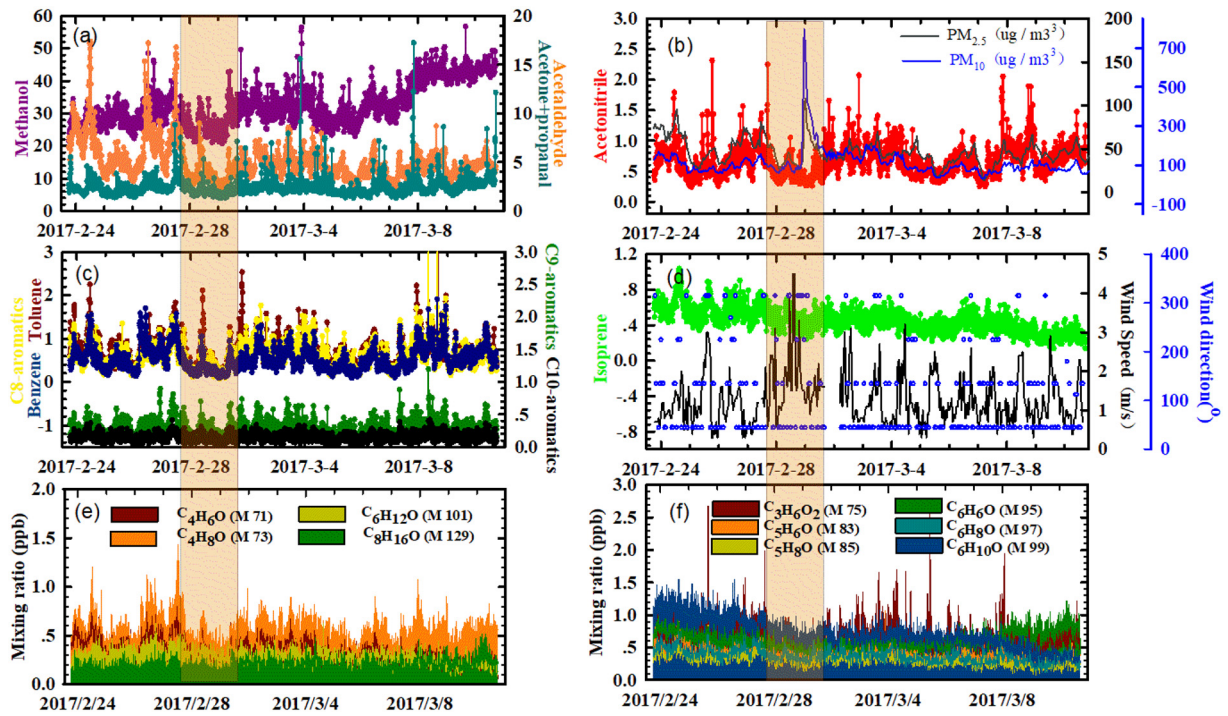


**Fig. 2.** Time series of 10 min temporal resolution data for the measured compounds. (a)methanol, acetaldehyde and acetone + propanal, (b)acetonitrile and PM, (c)aromatics VOCs: benzene, toluene, C8-aromatics (e.g., xylenes and ethylbenzene), C9-aromatics (e.g. trimethylbenzenes and propylbenzenes) and C10-aromatics (e.g., methylethylbenzenes), (d)isoprene and wind speed, (e) and (f) some OVOCs (C<sub>n</sub>H<sub>m</sub>O<sub>k</sub>: ketones/aldehydes/acids/formates/acetates/hydroxyketones/hydroxyaldehydes).

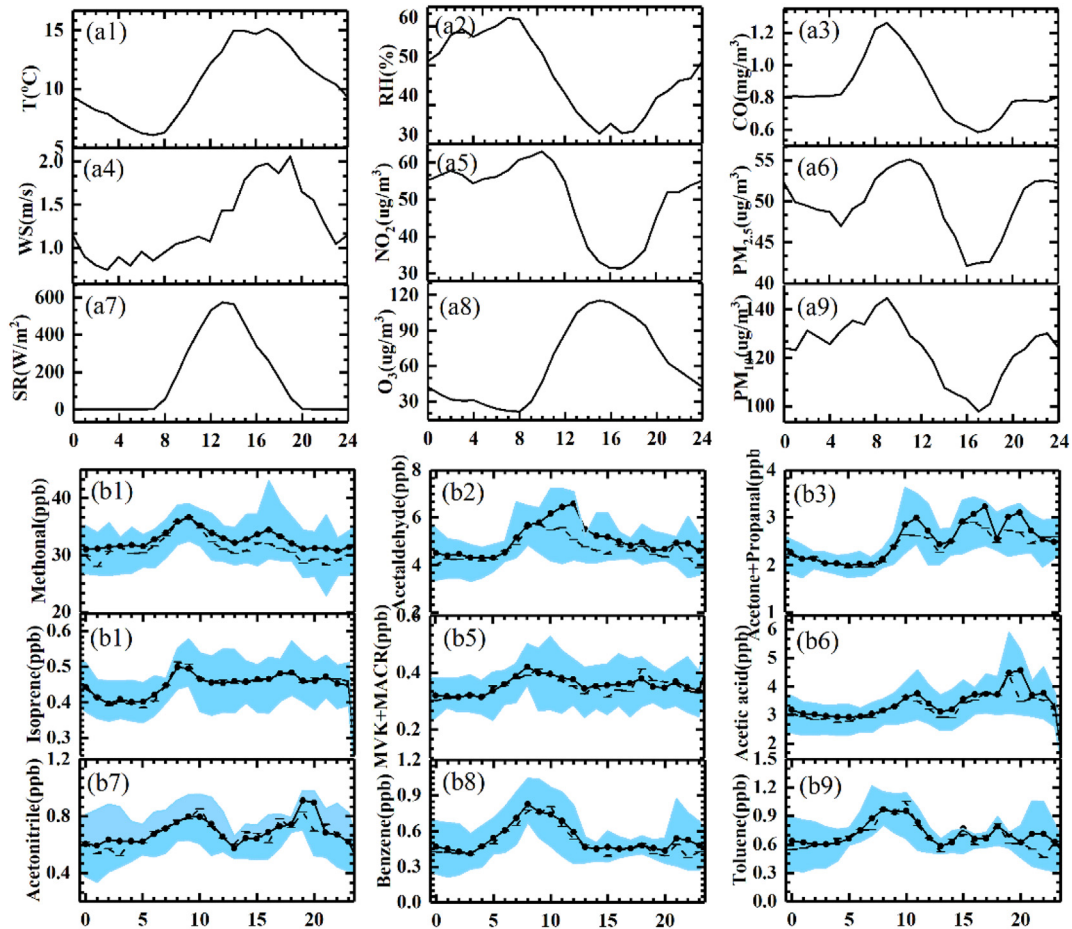


**Fig. 3.** (a) Other pollutants, meteorological parameter and (b) VOCs diurnal patterns at Lanzhou Valley. In part (b), the blue regions represent the interquartile range. The average value is shown with solid lines, dashed lines present the median values. (For interpretation of the references to color in this figure legend, the reader is referred to the web version of this article.)

northwest while mean wind speed was 1.12 m/s during nondust periods (Fig. 2d). VOCs might be affected by high wind speeds and turbulent mixing processes during dust periods, but the interaction between VOCs and wind speeds need further investigation. In Fig. 4, VOC mixing ratios except isoprene were lower in dust periods than in nondust periods. Benzene and methanol have the maximal two change rates with 53% and 30%, respectively. However, isoprene did not change during dust and nondust periods, suggesting isoprene, the biomarker for biologic emission, might have little influence from the dust variation.

Fig. 3a shows the diurnal variations of the other pollutants ( $\text{NO}_2$ , CO,  $\text{O}_3$ ,  $\text{PM}_{2.5}$  and  $\text{PM}_{10}$ ) and meteorological parameters (T, RH, WS and radiation) derived from the measurements. The solar radiation profile indicates that sunrise typically occurred at 07:00 LT, while sunset typically occurred at 20:00 LT. The mean values for  $\text{O}_3$ , T, WS and solar radiation were similar for the day with a unimodal profile characteristic that the maximum was at 16:00 LT for  $\text{O}_3$ , T, WS, while it was at 13:00 for solar radiation. In contrast, CO,  $\text{PM}_{2.5}$ ,  $\text{PM}_{10}$ ,  $\text{NO}_2$ , and RH have the lowest values at 16:00 LT; meanwhile, CO,  $\text{PM}_{2.5}$  and  $\text{PM}_{10}$  showed a bimodal profile characteristic with the effects of more urban activities emissions in the morning (08:00–09:00 LT) and the evening (21:00–22:00 LT). The evolution of the daytime atmospheric boundary layer height (ABLH) (Fig. S6) predicted it was 200 m at 08:00 LT, increasing until 1250 m at 17:00 LT, indicating that after 08:00 until 17:00 LT, decreases of the pollutants were observed due to the dilution effect exerted by the growing daytime boundary layer. However, for  $\text{O}_3$ , a secondary pollutant, despite the ABLH increase by 6 times, chemical production or transport of  $\text{O}_3$ -rich air sustained a net increase of  $88 \mu\text{g}/\text{m}^3$  from 08:00 to 16:00 LT, then decreased from 16:00 LT until midnight.

Fig. 3b analyzed the diurnal variations of VOCs including methanol, acetaldehyde, acetone + propanal, methyl vinyl ketone and methacrolein (MVK + MACR), isoprene, acetonitrile, acetic acid, benzene and toluene. All the VOCs exhibited bimodal patterns (morning and evening maxima) in a certain degree with the exception of isoprene, MVK + MVCR and acetaldehyde, which revealed the combined influence of urban traffic activities and biomass burning emissions. Acetone + propanal, acetic acid and acetonitrile had a bimodal diel profile (Fig. 3b3, b6, b7) with one peak at approximately 10:00 LT and another peak at 20:00 LT. While methanol had a diurnal pattern similar to the several VOCs, it peaked at approximately 10:00 LT and 16:00 LT. Such a bimodal pattern normally arises with two peaks due to the mixture of morning and evening emissions into a narrow ABLH, while it

reduces in the afternoon because pollution emissions were diluted by a fast-growing ABL for the heat flux in the troposphere. Aromatic VOCs such as benzene and toluene (Fig. 3b8, b9) displayed diurnal cyclical features of traffic emissions, with one peak in the morning rush hour 08:00 LT and a peak in the evening at 21:00 LT. Acetaldehyde's mixing ratios (Fig. 3b2) decreased during the nighttime and were high in the afternoon with a maximum at approximately 10:00 LT. The concentrations of isoprene and MVK + MVCR increased from 13:00 to 22:00 LT (Fig. 3b4, b5), having one peak at 08:00 LT. Isoprene, which is known to be emitted from terrestrial plants during the daytime presents the unimodal diurnal pattern consistent with vegetative and solar radiation, while the bimodal pattern was not observed for acetaldehyde, which was emitted by biomass burning and produced photochemically from precursor compounds (Roberts et al., 2014; Stockwell et al., 2015).

### 3.1.2. Comparison with VOC mixing ratios elsewhere

Fig. 4 shows a comparison of VOC mixing ratios in the Lanzhou Valley with VOC mixing ratios reported at urban environments elsewhere in the world (measured by a PTR-MS). OVOCs such as methanol (32.72 ppb) and acetaldehyde (5.05 ppb) in the Lanzhou Valley were higher than in other cities except as reported in Mohali and Kathmandu (Sinha et al., 2014; Sarkar et al., 2016). In contrast, Lanzhou had lower aromatics levels (benzene, toluene and C8-aromatics) compared with most other cities where industrial and traffic sources are much larger than Lanzhou. Acetonitrile (0.45 ppb) and isoprene (0.69 ppb) were lower than measured in Ahmedabad (Sahu et al., 2016), Kathmandu (Sarkar et al., 2016), Mohali (Sinha et al., 2014) and Barcelona (Stojić et al., 2015), most of which are in India. Furthermore, acetonitrile was lower than what was measured in Paris (Alexia et al., 2016) while isoprene was lower than levels in Athens (Kaltsonoudis et al., 2016). Wintertime measurements in Helsinki in Finland (Rantala et al., 2016) and New Hampshire in America (Jordan et al., 2009) suggest the air is much cleaner for many of the VOCs. High ambient concentrations within the Lanzhou Valley cities (which results in suppressed diffusion) for several OVOCs—such as acetaldehyde, acetonitrile and isoprene—appear on account of the strong oxidizing environment such as long sunshine duration and strong solar radiation due to its high altitude and less wet deposition due to in the semiarid region. Meanwhile low concentrations for benzenoids might be related to much smaller population densities, traffic and industries compared to megacities such as Tokyo (Yoshino et al., 2012), Guangzhou (Liu et al., 2008a) and YRD (Pan et al., 2015) in Asia. On the

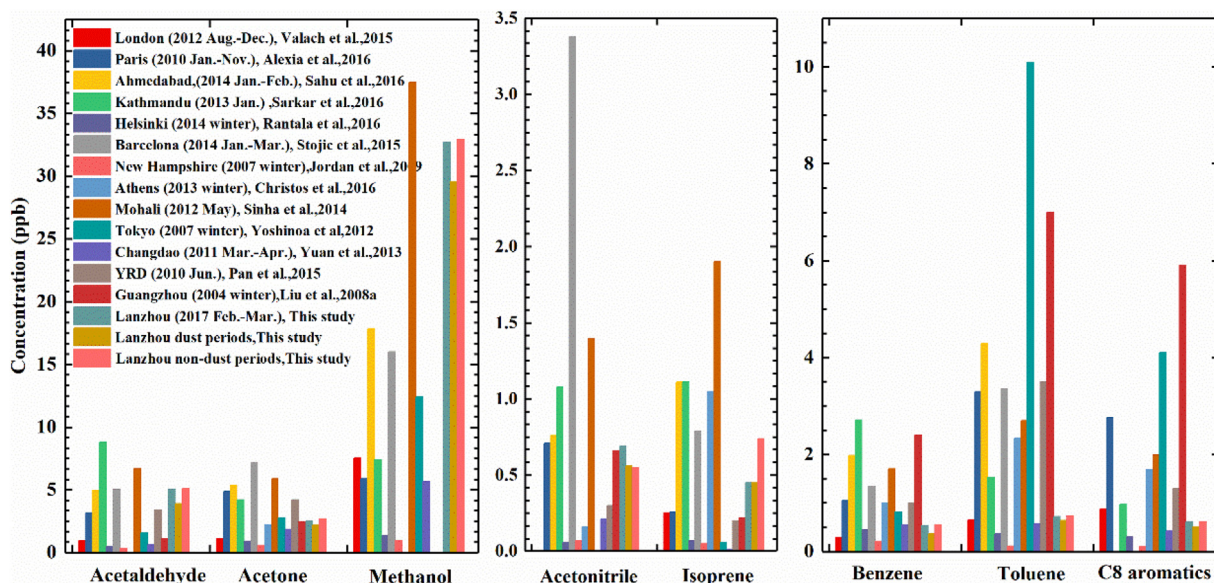


Fig. 4. Comparison of VOC mixing ratios measured in Lanzhou Valley (mean, dust and non-dust periods) with VOC levels at other urban sites in the world (measured by PTR-MS).

other hand, several possible reasons exist for lower concentrations of benzenoids in the typical petrochemical industrialized valley city. First, the sampling site was in an urban community in Chengguan district, not in the petrochemical industries areas in Xigu district; second, favorable meteorological conditions during these PTR-MS measurement periods probably resulted in lower concentrations in Lanzhou. The wind direction in these periods were basically NNE and NE (Fig. 1), which is the opposite direction of the petrochemical industries to the sampling site. Meanwhile, higher wind speeds in the dust source area in spring might enhance the diffusion of benzenoids.

### 3.1.3. Ratios analysis

Emission ratios (ERs, Table 1) equal  $\Delta[\text{VOCs}]/\Delta\text{CO}$ , where  $\Delta[\text{VOCs}]$  is the difference of VOC mixing ratios between the biomass burning period (8 March) and the adjacent reference period. The adjacent period was chosen on the basis of the low acetonitrile and CO concentrations levels, which was before and after the burning period. In this study, ERs (residential activities) of OVOCs such as formic acid, acetic acid, MVK + MACR and MEK were lower than residential heating (Kaltsonoudis et al., 2016), SE, SW and pine spruce fuels (Warneke et al., 2011), African grass and Alfalfa (Stockwell et al., 2015). Acetone was lower than the values reported above except SW fuels and African grass. Biogenic ERs such as isoprene are lower than the values above, while monoterpenes are lower than all of the values except African grass. ERs of acetonitrile were greater than the values above except Alfalfa. Benzenoids' ERs were greater than SE, SW fuels (Warneke et al., 2011) and African grass fuels (Stockwell et al., 2015).

Benzene to toluene (B/T) ratios can identify source types, and the changes of B/T ratios can indicate the photochemical age of an air mass because toluene reacts with OH at a faster rate (toluene:  $k_{\text{OH}} = 5.6 \times 10^{-12} \text{ cm}^3 \text{ molecule}^{-1} \text{ s}^{-1}$ ; benzene:  $k_{\text{OH}} = 1.2 \times 10^{-12} \text{ cm}^3 \text{ molecule}^{-1} \text{ s}^{-1}$ ), assuming sufficient OH concentrations to drive the reaction (Roberts et al., 1984; Kristensson et al., 2004; Warneke et al., 2007; Marc et al., 2014). B/T ratios within the range of 1.5–2.2 are considered an indicator of coal combustion (Wang et al., 2013). A specific B/T ratio below 0.2 has been proposed and used as an indicator of samples strongly affected by solvent use (Barletta et al., 2008). B/T ratios of approximately 0.6 were characterized by traffic emissions worldwide (Barletta et al., 2005). In this study, the mean B/T ratio was 0.7 (wt/wt), and evaporative emissions from gasoline or direct industrial toluene emissions are considered to contribute to the lower B/T ratios in Lanzhou. WS and WD play an important role in the change of B/T ratios by transporting pollution over longer distances, allowing more time to react with OH or exposure to higher OH concentrations, thus increasing the ratio. Fig. 5 is an example, and it was seen on 28 February when mean B/T ratios reached 0.84 with stronger NW winds (mean  $2.14 \text{ ms}^{-1}$ ), possibly advecting pollution from Tibet Plateau and Hexi

Corridor. Meanwhile on 5 March mean B/T ratios were 0.65 with low WS (mean  $1.02 \text{ ms}^{-1}$ ), indicating higher contributions of near sources such as local urban emission. The back trajectories indicated air mass had passed over Tibet Plateau and Hexi Corridor in the past 24 h during periods of high B/T ratios, due to longer distances allowing more time to react with OH concentrations and clean air being exposed to lower OH concentrations. Mean concentration ratios for benzene to C8-aromatics were 0.89 and for toluene to C8-aromatics were 1.18, which both suggest these masses are the ascribed traffic-related compounds (Corrêa and Arbilla, 2006; Valach et al., 2015).

## 3.2. Sources of VOCs in the Lanzhou Valley

### 3.2.1. PMF model to identify source factors

Eight sources were identified using PMF for the initial mixing ratio of VOC as follows: (1) mixed industrial process-1 (13.50%), (2) secondary formation (13.15%), (3) mixed industrial process-2 (11.84%), (4) residential biofuel use and waste disposal (13.80%), (5) solvent usage (10.14%), (6) vehicular exhaust (11.81%), (7) biogenic (13.77%), and (8) biomass burning (12.00%). Source profiles and the contribution percentage of factors are shown in Fig. 6. The correlation analysis has much higher R values for the top 2 or 3 compounds explained by each factor (Table S3), and the normalized time series and diurnal variation for the 8 factor sources were shown in the Fig. S7.

The main species in the profile of factor 1 were butyric acid (28.3%), Formic acid and ethanol (20.2%), acetone (29.7%) and hydroxy acetone (35.05%). Meanwhile, the profile for factor 3 consists of 1,3-butadiyne (29.3%) and butyric acid (32.5%), which are used in the production of several polymers and some spices and are the main ingredients emitted from the chemical industry. Moreover, approximately 15–25% of the propyne, acetonitrile, propene and methyl furan were in the two factors. In addition, the compounds above are frequently present in a variety of industrial emissions sources (Watson et al., 2001; Kim et al., 2008). Therefore, both factors were identified as mixed industrial process. However, the two factors have significant differences. Factor 3 had considerably high levels of styrene (26.5%), trimethylbenzenes (26.0%), and C10-aromatics (11.8%), which were often used as a solvent and originated from unburned liquid gasoline (USEPA, 1994; Li et al., 2016). Factor 1 had higher levels of benzene (14.7%) and methyl furan (19.1%) than factor 3 did, two chemicals emitted during coal-burning processes. Thus, factor 1 is associated with mixed industrial processes principally in the combustion or reaction industry, and factor 2 is related to mixed industrial processes principally in the chemical solvent industry.

Factor 2 explained acetone (43.1%), acetic acid (22.5%), acetamide (10.8%) and phenol (19.0%). The factor has a predominance of oxygenated compounds probably on account of photooxidation and was contributed less from VOCs such as acetonitrile and propyne, which were

**Table 1**  
Emission ratios with urban activities. Comparison with the measurement ERs from various types.

| Emission ratios ( $\Delta\text{VOCs}/\Delta\text{CO}$ , ppbv/ppmn) |                                  |  |                                    |                                    |  |  |                                     |
|--|----------------------------------|--|------------------------------------|------------------------------------|--|--|-------------------------------------|
| Species  | Urban activities<br>(This study) | Residential heating<br>(Kaltsonoudis et al., 2016) | SW fuels (Warneke<br>et al., 2011) | SE fuels (Warneke<br>et al., 2011) | Pine spruce<br>(Warneke et al.,<br>2011) | African grass<br>(Stockwell et al.,<br>2015) | Alfalfa (Stockwell<br>et al., 2015) |
| Acetonitrile   | 1.13 ± 0.45                      | 0.32 ± 0.05  | 0.56                               | 1.03                               | 1.05                                     | 0.50 ± 0.39                                  | 6.0 ± 0.9                           |
| Formic acid + ethanol  | 0.70 ± 0.20                      | 1.3 ± 0.3  | 0.77                               | 1.08                               | 1.0                                      | 1.65 ± 0.81                                  | 1.08 ± 1.29                         |
| Acetone  | 1.70 ± 1.32                      | 2.9 ± 0.5  | 0.84                               | 1.93                               | 1.94                                     | 1.19 ± 1.42                                  | 5.2 ± 0.5                           |
| Acetic acid  | 0.16 ± 0.24                      | 2.0 ± 1.0  | 4.84                               | 13.61                              | 8.19                                     | 13.2 ± 6.8                                   | 31 ± 6.8                            |
| Isoprene   | 0.23 ± 0.04                      | 1.6 ± 0.22   | 0.53                               | 1.38                               | 1.57                                     | 0.33 ± 0.27                                  | 2.3 ± 0.1                           |
| MVK + MACR   | 0.13 ± 0.03                      | 0.7 ± 0.1  | 0.43                               | 1.08                               | 1.32                                     | 1.11 ± 0.94                                  | 1.6 ± 0.3                           |
| MEK  | 0.25 ± 0.07                      | 0.7 ± 0.2  | 0.41                               | 1.28                               | 1.17                                     | 0.26 ± 0.22                                  | 1.5 ± 0.3                           |
| Benzene  | 1.37 ± 0.21                      | 1.8 ± 0.2  | 0.86                               | 0.83                               | 2.29                                     | 0.57 ± 0.3                                   | 2.5 ± 1.1                           |
| Toluene  | 1.41 ± 0.46                      | 3.3 ± 0.8  | 0.30                               | 0.48                               | 0.81                                     | 0.3 ± 0.2                                    | 1.8 ± 0.1                           |
| C <sub>8</sub> -Aromatics  | 1.42 ± 0.31                      | 2.8 ± 0.6  | 0.19                               | 0.35                               | 0.60                                     | 0.07 ± 0.04                                  | 0.5 ± 0.04                          |
| Monoterpenes   | 0.15 ± 0.02                      | 0.7 ± 0.2  | 0.16                               | 0.55                               | 1.25                                     | 0.004 ± 0.002                                | 0.33 ± 0.03                         |

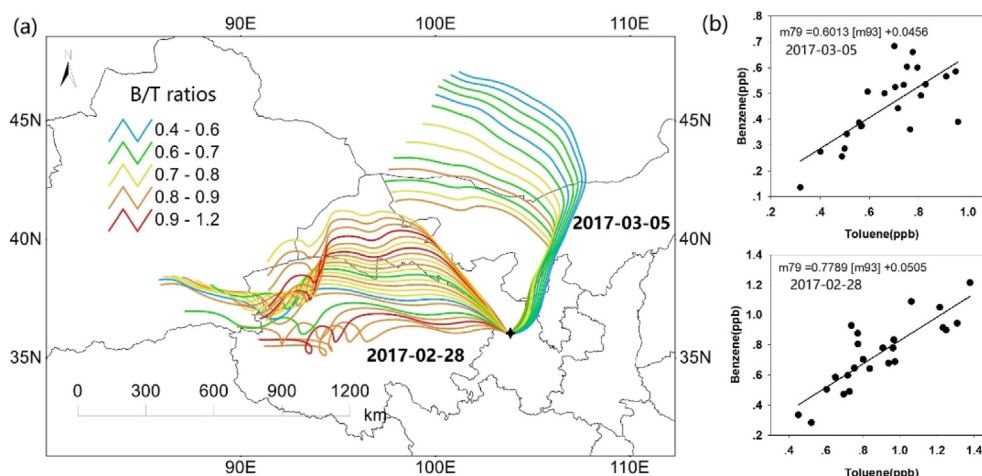


**Fig. 5.** (a) 24 h back trajectories from the NOAA HYSPLIT trajectory model on 28 February and 5 March 2017 respectively related to periods of high and low B/T ratios, back trajectories were run at 3 h intervals starting at ground-level (500 m) from Lanzhou and propagated 24 h backwards in time. (b) scatter plots showing B/T ratios on 28 February 2017 (top) and 5 March 2017 (bottom).

primary species emitted from industrial emissions and biomass combustion (Akagi et al., 2011). Therefore, this factor was named secondary formation. Factor 4 was mainly associated with methyl furan (35.5%) and furfural (33.49%). Garbage and/or trash burning activities were intense in the Lanzhou Valley, which can release furan into the atmosphere (Klimont et al., 2002). This factor was also characterized by large numbers of aldo ketones, such as acrolein (37.1%), cyclopentanone (33.4%), hexenal (51.45%), hexanal (29.7%) and styrene (25.3%), which are major emission sources from burning processes (Liu et al., 2008a). Hence, this factor was identified as residential biofuel use and waste disposal.

Factor 5 was identified as solvent usage with abundant aromatics such as xylenes (60.31%), trimethylbenzenes (32.8%), and C10-aromatics (29.3%) ( $R^2 > 0.7$ , Table S3). Those species were usually used in coatings, paints, inks, and cleaning agents (Borbon et al., 2002; Liu et al., 2008b; Sun et al., 2016), which originated from unburned liquid gasoline and were used widely as a chemical tracer of solvent utilization (Karl et al., 2003; Yan et al., 2017). However, we found that Factor 5 solvent usage contributed less (2.5%) to benzene compared to Factor 3, mixed industrial process-2 (9.5%). As benzene was the most abundant species for the chemical and paint industries but was strictly prohibited in residential solvent usage in China (Yuan et al., 2010), we deduced that Factor 5 solvent usage with lower values of benzene was relatively less oil industry-related. High percentages of benzene (57.1%) and toluene (44.6%) were obtained in Factor 6, which was identified as vehicle-related. Acetone (27.1%) and acetaldehyde (22.5%) was added to the factor mass. Good correlations were found between benzene and toluene ( $R^2 = 0.80$ ), as well as with acetaldehyde with  $R^2 = 0.68$  for benzene and with  $R^2 = 0.60$  for toluene, suggesting common vehicle emission sources.

Factor 7 was a biogenic emissions source containing a particularly large content of isoprene (45.4%) and monoterpene (35.1%), indicators of biogenics. The correlation coefficient between isoprene and monoterpene was 0.48. In this factor, most of the VOCs mass was related to OVOCs, such as MVK + MACR (48.2%), acetaldehyde (25.9%) and MEK (21.7%). The primary oxidation products of isoprene are MVK + MACR (White et al., 2008), and a portion of isoprene was emitted by traffic sources in urban areas (Hellén et al., 2012). Toluene (26.0%) was observed in this study, which suggested traffic probably has some influence in  $m/z69$   $C_5H_8H^+$ . A recent study suggested  $m/z69$   $C_5H_8H^+$  could also result from the fragmentation of cycloalkanes and cycloalkenes (Millet et al., 2008; Gueneron et al., 2015). Compounds fragmentation could lead to productions at  $m/z111$ , and the masses signal (at 135 Td) could be above 0.2 ppb, in view of the fragmentation

form  $m/z69$   $C_5H_8H^+$  ion signal in the observed mass spectra. The signal at  $m/z111$  was 0.25 ppb (above 0.2 ppb); thus, we deduce isoprene is the unconventional assignment. Acetonitrile (30.6%) and propanenitrile (43.8%) made the most contribution to the VOCs mass of Factor 8. Farmers burn large numbers of biomass, crop residue and wood in the early spring (Millet et al., 2010; Akagi et al., 2011), which can result in important emissions of biomass burning tracers (Stone et al., 2010).

### 3.2.2. CPFs to determine local source directionality

Via conditional probabilities function (CPF) analyses, 8 factor–source categories could be identified corresponding to different physical orientations (Kim et al., 2005). Fig. 6 illustrated the directional dependence of the origins in the Lanzhou Valley. CPF plots indicated the mixed industrial process-1 mainly originated from the SE direction with conditional probability (CP) values of approximately 0.4, associated with the locations of the LanRe industrial estate including a coal-fired power plant. CP values were observed for the NE and SW directions where a few industries are located. The secondary formation factors clearly indicated the highest CP values of air masses reaching the measurement site were from the NE to SE wind sectors ( $p = 0.3–0.5$ ). The mixed industrial process-2 displayed higher contributions from the W direction ( $p = 0.3–0.95$ ), associated with the locations of the petrochemical industry in Xigu district. The CPF plots for residential biofuel use and waste disposal sources indicated the source was located to the NE to SE directions ( $p = 0.2$  to  $0.3$ ), which is related to compact residential areas with more human activity. CPF results for the solvent usage sources showed the source was associated with the W direction ( $p = 0.4$  to  $0.95$ ), and slightly higher CP values ( $p = 0.45$ ) are recorded with air masses reaching this site from the NW and SW directions. These CPF plots overlap with the CP values of the mixed industrial process-2 factor, which suggests the solvent usage from other emissions areas (mainly residential regions) also contributed to this factor. For vehicular exhaust, the CP values were related to all directions, but the highest CP values were from the NW and the SE directions ( $p = 0.5$ ), where the Lanzhou city center, the busiest commercial district and transportation junction, was located. High values for biogenic sources were observed from the NW direction ( $p = 0.2$  to  $0.4$ ), where several forested regions with flourishing vegetation, such as Baita mountain and near the reserve forest, were located. The biomass burning factor showed high CP values for air masses reaching the measurement site from the S and SE direction ( $p = 0.95$ ), where a few active farming groups were located near the suburban areas of city.

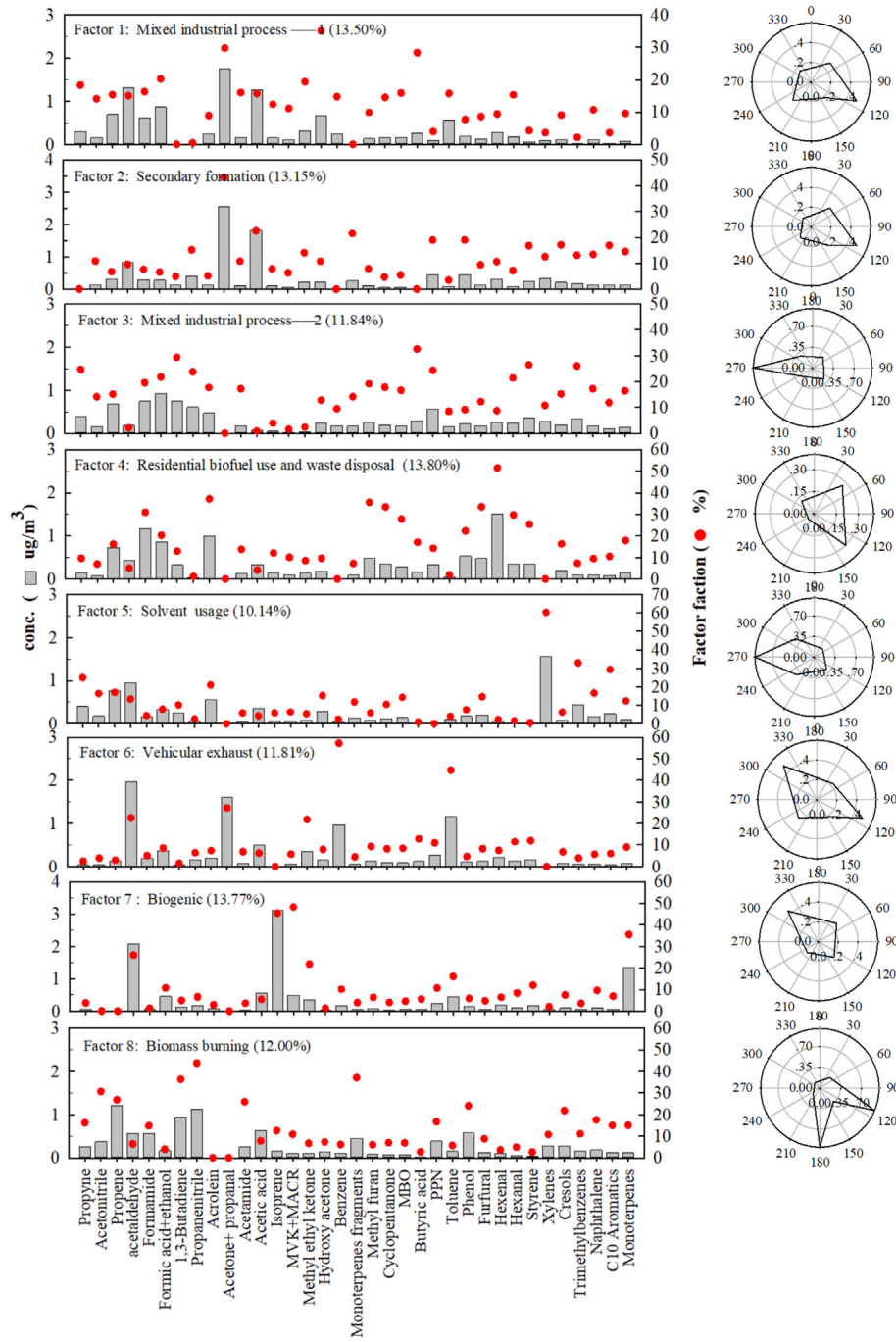


**Fig. 6.** VOC profiles of identified sources from the PMF model (grey bar is the concentration and red dot is the percentage) and their CPF plots. (For interpretation of the references to color in this figure legend, the reader is referred to the web version of this article.)

**Table 2**

Average concentrations (ppbv) of six sources for different air mass arriving in Lanzhou site and contribution (%) of near- and far-regional sources. (The concentrations greater than 1.0 were bold and italic).

| Air mass type      | Mixed industrial process-1 | Mixed industrial process-2 | Residential biofuel use and waste disposal | Solvent usage | Vehicular exhaust | Biomass burning |
|--------------------|----------------------------|----------------------------|--|---------------|-------------------|-----------------|
| Cluster1(ppbv)     | 0.88                       | 0.76                       | <b>1.28</b>                                | <b>1.02</b>   | 0.83              | <b>1.33</b>     |
| Cluster2(ppbv)     | 0.85                       | <b>1.11</b>                | <b>1.17</b>                                | <b>1.12</b>   | <b>1.12</b>       | 0.86            |
| Cluster3(ppbv)     | <b>1.69</b>                | 0.81                       | 0.77                                       | 0.66          | 0.61              | 0.44            |
| Cluster4(ppbv)     | 0.43                       | 0.72                       | <b>1.38</b>                                | <b>1.03</b>   | <b>1.54</b>       | 0.58            |
| Distant source (%) | 33.03                      | 32.25                      | 30.72                                      | 35.01         | 28.90             | 35.13           |
| Local source (%)   | 66.97                      | 67.75                      | 69.28                                      | 64.99         | 71.10             | 64.87           |

### 3.2.3. Air trajectory analysis to determine regional near- and far-source contribution

Backward trajectory cluster has been widely used to demonstrate the transport pathways of air masses, and a raster analysis based on the PSCF and CWT models were applied to identify the source areas of VOCs during monitoring periods. To quantify the source concentrations from different air masses as well as the contributions of regional near-sources and long-range transport to the sampling site, trajectory cluster and sector analyses based on CWT were applied, the results of which are summarized in Table 2. The Lanzhou site had 4 major air mass transport trajectories according to their directions and transport areas (Fig. S4). Trajectory 1, 2, 3 and 4 accounted for 26.18%, 39.28%, 14.21% and 20.33% of all the trajectories, respectively. Trajectory 1 was derived from Gansu province (southeast of the Lanzhou Valley) with a short transport pattern, while trajectory 2 began from Sinkiang (west of the Lanzhou Valley), passing over Qinghai province. Trajectory 3 originated from south of Mongolia (north and northeast of the Lanzhou Valley), passing through Inner Mongolia, and trajectory 4 was from southwest

of Mongolia (northwest of the Lanzhou Valley), passing the edge of Badain Jaran Desert before arriving at Lanzhou. All trajectories involved long transport patterns.

Except for secondary formation and biogenic sources, of which major emitted compounds have a shorter life span, VOCs source regions of six factors from PMF model (i.e., mixed industrial process-1, mixed industrial process-2, residential biofuel use and waste disposal, solvent usage, vehicular exhaust and biomass burning) apportioned by the PSCF and CWT models are presented in Fig. 7. Both the PSCF and the CWT results of mixed industrial process-1 were mainly from the northeast of the Lanzhou Valley, near Ningxia province, where a large quantity of heavy industries are distributed. Meanwhile, the mixed industrial process-1 source level consistent with cluster 3 was highest with 1.69 ppb (Table 2), suggesting the air mass from the northeast might carry pollutants in the heavy industries areas and impact the air quality of the Lanzhou Valley. Both the PSCF and the CWT results of biomass burning were mainly from southeast of the Lanzhou Valley, which was related to the large areas of crop residue burning (straw or wheat)

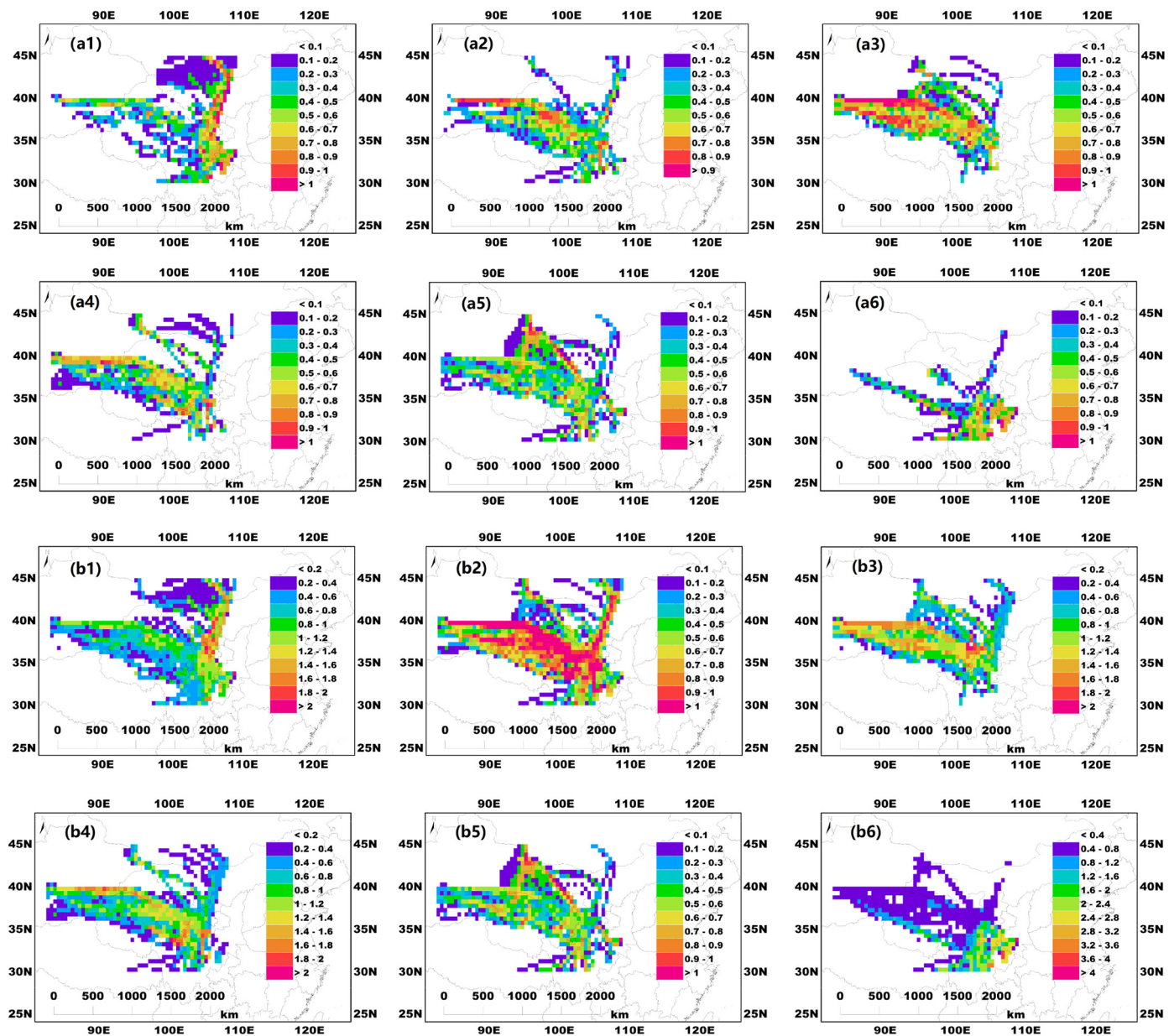


Fig. 7. Results of (a) the WPSCF and (b) the WCWT maps with six sources derived from PMF model: (1) mixed industrial process-1, (2) mixed industrial process-2, (3) residential biofuel use and waste disposal, (4) solvent usage, (5) vehicular exhaust and (6) biomass burning.

derived from the analysis of the MODIS fire count data (Fig. S8) for the measurement periods, revealing crop residue burning was quite widespread in the upwind regions and was the likely cause for the extremely high plume values. Meanwhile, the biomass burning source level consistent with cluster 1 was highest with 1.33 ppb (Table 2), suggesting the air mass from the north and northeast of the Lanzhou Valley might carry the gaseous product of combustion from the crop burning areas. However, the PSCF and the CWT results of the other four factors (mixed industrial process-2, residential biofuel use and waste disposal, solvent usage and vehicular exhaust) sources were mainly from the west and the northwest of the Lanzhou Valley, which was associated with the dust area of the Gobi Desert, and some from the southwest, which was probably because of the fire point. Those four-sources levels were related to clusters 2 and 4 with >1 ppb, which originated from the northwest and the west of the Lanzhou Valley. A trajectory sector analysis (Table 2) revealed that the local source contributed most to vehicular exhaust (71.10%) and residential biofuel use and waste disposal (69.28%) for the short-distance transport, while the lowest contributions of the biomass burning (64.87%) and solvent usage (64.99%) were observed.

### 3.3. Reactive chemicals

#### 3.3.1. The effects of VOCs on ozone formation potential

The VOCs contributing the most to the OH reactivity are listed in Table S4. Contributions of acetaldehyde, Propene and 1,3-Butadiene to average OH reactivity are all >10%, and many contributors are strong biomass combustion sources emissions. Fig. 8a shows the eight PMF-

derived source contributions to OFP while Fig. 8b shows the contributions of different chemical groups of compounds measured in the Lanzhou Valley to OFP. The OFP of VOCs was 3.66 ppb/h; OVOCs accounted for 43% of the OFP; and isoprene, benzenoids and nitriles/furans accounted for 9%, 9% and 12%, respectively. In the OVOCs group, acetaldehyde (35%), methanol (14%) and acrolein (11%) were the top 3 contributors, and styrene (40%) contributed most to the OFP of benzenoids group, while in the nitriles/furans group, methyl furan was the top contributor accounting for 66%. Propene and 1,3-Butadiene in the others group contributed most to the OFP, with proportions of 51% and 44%, respectively. In Fig. 8a, residential biofuel use and waste disposal, mixed industrial process-2 and solvent usage appeared to be the dominant contributors to O<sub>3</sub> production, accounting for 25.1%, 15.3% and 13.4%, respectively.

#### 3.3.2. Contributions of VOCs to SOA formation

The SOA yield of a specific VOC depends on the NO<sub>x</sub> conditions due to the competition reactions of the RO<sub>2</sub> radical with the NO and HO<sub>2</sub> radical (Bahreini et al., 2009; Henze et al., 2008). The SOA yields of most benzenoids at high-NO<sub>x</sub> conditions are significantly lower than those at low-NO<sub>x</sub> conditions (Ng et al., 2007). Hence, we calculated SOAF from VOC oxidations under high- and low-NO<sub>x</sub> conditions, which represented the higher and lower limits of SOA formed in this work. The literature showed the aromatics accounted for 97.5% and 91.9% of the SOAF from VOC oxidations under low- and high-NO<sub>x</sub> conditions, respectively (Yuan et al., 2013). In this study, VOC species that could contribute SOAF were principally aromatics (Table S1). Fig. 9a shows the contribution of individual VOCs to SOAF, while Fig. 9b

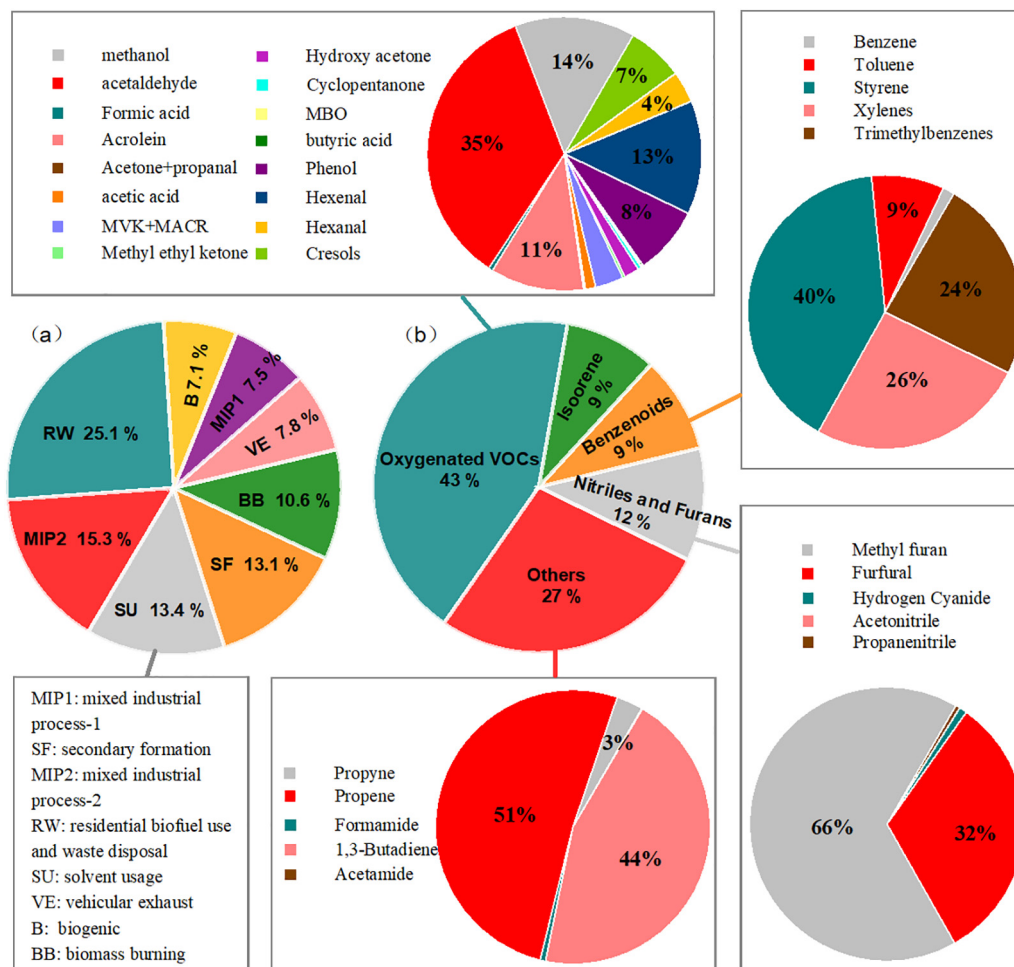
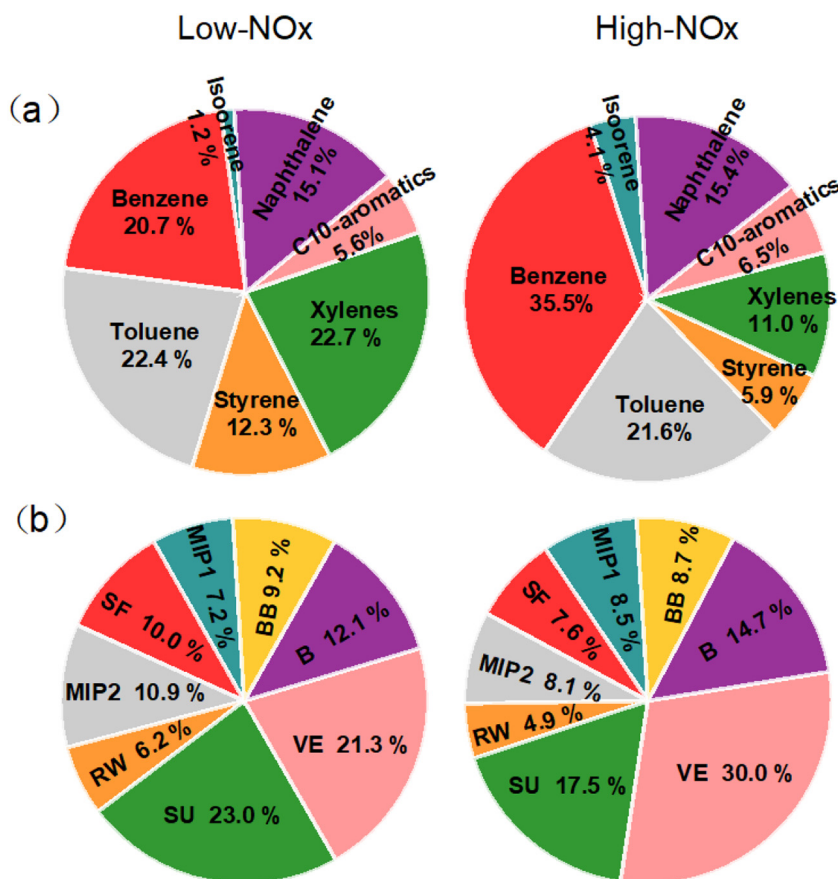


Fig. 8. Pie charts showing (a) contribution of 8 PMF-derived sources to OFP, and (b) contribution of classes of VOCs and individual VOCs to OFP.



**Fig. 9.** (a) Contribution of individual VOCs to SOA formation, (b) contribution of the 8-factor sources to SOA formation. Left is under low-NOx conditions, right is under high-NOx conditions. MIP1 is mixed industrial process-1, SF is secondary formation, MIP2 is mixed industrial process-2, RW is residential biofuel use and waste disposal, SU is solvent usage, VE is vehicular exhaust, B is biogenic and BB is biomass burning.

shows the contribution of the 8 factor sources to SOAF. The rank of main SOAF precursors under low-NOx conditions is xylene > toluene > benzene > naphthalene > styrene > C10-aromatics > isoprene, while under high-NOx conditions, it is benzene > toluene > naphthalene > xylene > C10-aromatics > styrene > isoprene. As the solvent usage and vehicular exhaust contain most of the reactive aromatic compounds, they appeared to be the dominant contributors to SOAF in the Lanzhou Valley.

#### 4. Conclusion

Real-time monitoring of VOCs in the Lanzhou Valley was implemented to improve our understanding of the VOCs levels and variabilities, to identify their major origins and potential regions, as well as to assess the contributions of individual VOCs and their PMF-derived sources to O<sub>3</sub> and SOA. The VOC mixing ratios ranking was methanol > acetaldehyde > acetic acid > propene > acetone + propanal > formic acid + ethanol > toluene > sum of C8-aromatics. VOCs might be affected by high wind speeds and turbulent mixing processes during dust periods. Higher OVOCs with lower aromatics levels in the Lanzhou Valley were found compared with most other cities.

The PMF solution was to divide VOCs into 8 sources as follows: mixed industrial process-1, secondary formation, mixed industrial process-2, residential biofuel use and waste disposal, solvent usage, vehicular exhaust, biogenic and biomass burning. The CPF analysis indicated spatially stationary origins are responsible for an important fraction of the observed VOC mass loadings. Both the PSCF and the CWT results of mixed industrial process-1 were mainly from the northeast of the Lanzhou Valley, near Ningxia province, where a large quantity of heavy industries is distributed. Biomass burning was mainly

from the southeast of the Lanzhou Valley, which was related to the large areas of crop residue burning, while mixed industrial process-2, residential biofuel use and waste disposal, solvent usage and vehicular exhaust sources were mainly from the west and the northwest of the Lanzhou Valley, which were associated with the dust area of the Gobi Desert, and some from the southwest. The trajectory sector analysis revealed that the local source contributed most to vehicular exhaust (71.10%) and residential biofuel use and waste disposal (69.28%).

OVOCs accounted for 43% of OFP, and isoprene, benzenoids and nitriles/furans accounted for 9%, 9% and 12%, respectively. Residential biofuel use and waste disposal, mixed industrial process-2 and solvent usage appeared to be the dominant contributors to O<sub>3</sub> production. The rank of main SOA precursors under low-NOx conditions is xylene > toluene > benzene > naphthalene > styrene > C10-aromatics > isoprene, while under high-NOx conditions is toluene > naphthalene > xylene > C10-aromatics > styrene > benzene > isoprene. Solvent usage and vehicular exhaust appeared to be the dominant contributors to SOAF in the Lanzhou Valley. This study first provided the quantitative information regarding the VOCs levels using a PTR-MS, the contributions of the major VOCs sources and the influence of VOCs on secondary pollutants in the Lanzhou Valley. This study could provide support for devising appropriate abatement strategies by policy makers and practitioners to improve the air quality of Lanzhou by reducing emissions of both toxic VOCs and the formation of secondary pollutants.

#### Acknowledgments

We thank the Qingyue Open Environmental Data Center (<https://data.epmap.org>) for providing air quality data. This work was supported by the foundation of the State Key Laboratory of Cryospheric Science

(SKLCS-ZZ-2019), the Strategic Priority Research Program of Chinese Academy of Sciences (Class A) (XDA20020102), the “Science Fund for Creative Research Groups of the National Natural Science Foundation of China” (41721091), the Strategic Priority Research Program of Chinese Academy of Sciences (class A) (XDA20060201), and the National Natural Science Foundation of China (41761134093, 41471058).

## Appendix A. Supplementary data

Supplementary data to this article can be found online at <https://doi.org/10.1016/j.scitotenv.2019.03.283>.

## References

- Akagi, S.K., Yokelson, R.J., Wiedinmyer, C., et al., 2011. Emission factors for open and domestic biomass burning for use in atmospheric models. *Atmos. Chem. Phys.* 11, 4039–4072. <https://doi.org/10.5194/acp-11-4039-2011>.
- Alexia, B., Valérie, G., Stéphane, S., et al., 2016. Seasonal variability and source apportionment of volatile organic compounds (VOCs) in the Paris megacity (France). *Atmos. Chem. Phys.* 16, 11961–11989. <https://doi.org/10.5194/acp-16-11961-2016>.
- Atkinson, R., 2000. Atmospheric chemistry of VOCs and NOx. *Atmos. Environ.* 34 (12–14), 2063–2101. [https://doi.org/10.1016/S1352-2310\(99\)00460-4](https://doi.org/10.1016/S1352-2310(99)00460-4).
- Atkinson, R., Arey, J., 2003. Atmospheric degradation of volatile organic compounds. *Chem. Rev.* 103 (12), 4605–4638. <https://doi.org/10.1021/cr0206420>.
- Atkinson, R., Baulch, D.L., Cox, R.A., et al., 2006. Evaluated kinetic and photochemical data for atmospheric chemistry: volume II – gas phase reactions of organic species. *Atmos. Chem. Phys.* 6 (11), 3625–4055. <https://doi.org/10.5194/acp-6-3625-2006>.
- Bahreini, R., Ervens, B., Middlebrook, A.M., et al., 2009. Organic aerosol formation in urban and industrial plumes near Houston and Dallas, Texas. *J. Geophys. Res.-Atmos.* 114, D00F16. <https://doi.org/10.1029/2008JD011493>.
- Bari, A., Dutkiewicz, V.A., Judd, C.D., et al., 2003. Regional sources of particulate sulfate, SO<sub>2</sub>, PM<sub>2.5</sub>, HCl, and HNO<sub>3</sub> in New York, NY. *Atmos. Environ.* vol. 37, pp. 2837–2844. [https://doi.org/10.1016/S1352-2310\(03\)00200-0](https://doi.org/10.1016/S1352-2310(03)00200-0).
- Barletta, B., Meinardi, S., Rowland, F.S., et al., 2005. Volatile organic compounds in 43 Chinese cities. *Atmos. Environ.* 39 (32), 5979e5990. <https://doi.org/10.1016/j.atmosenv.2005.06.029>.
- Barletta, B., Meinardi, S., Simpson, I.J., et al., 2008. Ambient mixing ratios of nonmethane hydrocarbons (NMHCs) in two major urban centers of the Pearl River Delta (PRD) region: Guangzhou and Dongguan. *Atmos. Environ.* 42 (18), 4393e4408. <https://doi.org/10.1016/j.atmosenv.2008.01.028>.
- Blake, R.S., Monks, P.S., Ellis, A.M., 2009. Proton-transfer reaction mass spectrometry. *Chem. Rev.* 109, 861–896. <https://doi.org/10.1021/cr800364q>.
- Borbon, A., Locoge, N., Veillerot, M., et al., 2002. Characterization of NMHCs in a French urban atmosphere: overview of the main sources. *Sci. Total Environ.* 292, 177e191. [https://doi.org/10.1016/S0048-9697\(01\)01106-8](https://doi.org/10.1016/S0048-9697(01)01106-8).
- Carter, W.P.L., Atkinson, R., 1989. Computer modeling study of incremental hydrocarbon reactivity. *Environ. Sci. Technol.* 23, 864–880. <https://doi.org/10.1021/es00065a017>.
- Chu, P.C., Chen, Y.C., Lu, S.H., et al., 2008a. Atmospheric effects on winter SO<sub>2</sub> pollution in Lanzhou, China. *Atmos. Res.* 89 (4), 365–373. <https://doi.org/10.1016/j.atmosres.2008.03.008>.
- Chu, P.C., Chen, Y.C., Lu, S.H., et al., 2008b. Afforestation for reduction of NOx concentration in Lanzhou China. *Environ. Int.* 34 (5), 688–697. <https://doi.org/10.1016/j.envint.2007.12.014>.
- Chu, P.C., Chen, Y.C., Lu, S.H., 2008c. Particulate air pollution in Lanzhou, China. *Environ. Int.* 34 (5), 698–731. <https://doi.org/10.1016/j.envint.2007.12.013>.
- Corrêa, S.M., Arbilla, G., 2006. Aromatic hydrocarbons emissions in diesel and biodiesel exhaust. *Atmos. Environ.* 40, 6821–6826. <https://doi.org/10.1016/j.atmosenv.2006.05.068>.
- de Gouw, J. and Warneke, C., 2007. Measurements of volatile organic compounds in the earth's atmosphere using proton-transfer-reaction mass spectrometry. *Mass Spectrom. Rev.* 26, 223–257. doi:<https://doi.org/10.1002/mas.20119>, 2007.
- de Gouw, J.A., Goldan, P.D., Warneke, C., et al., 2003. Validation of proton transfer reaction mass spectrometry (PTR-MS) measurements of gas-phase organic compounds in the atmosphere during the New England Air Quality Study (NEAQS) in 2002. *J. Geophys. Res.* 108 (D21), 4682. <https://doi.org/10.1029/2003JD003863>.
- Debevec, C., Sauvage, S., Gros, V., et al., 2017. Origin and variability of volatile organic compounds observed at an eastern Mediterranean background site (Cyprus). *Atmos. Chem. Phys.* 17 (18), 11355–11388. <https://doi.org/10.5194/acp-17-11355-2017>.
- Dimitriou, K., Kassomenos, P., 2015. Three-year study of tropospheric ozone with back trajectories at a metropolitan and a medium scale urban area in Greece. *Sci. Total Environ.* 502, 493–501. <https://doi.org/10.1016/j.scitotenv.2014.09.072>.
- Fleming, Z.L., Monks, P.S., Manning, A.J., 2012. Review: untangling the influence of air-mass history in interpreting observed atmospheric composition. *Atmos. Res.* 104–105, 1–39. <https://doi.org/10.1016/j.atmosres.2011.09.009>.
- Gueneron, M., Erickson, M.H., VanderScheld, G.S. et al., 2015. PTR-MS fragmentation patterns of gasoline hydrocarbons. *Int. J. Mass Spectrom.* 379, 97–109. <https://doi.org/10.1016/j.ijms.2015.01.001>.
- Hellén, H., Tykkä, T., Hakola, H., 2012. Importance of monoterpenes and soprene in urban air in northern Europe. *Atmos. Environ.* 59, 59–66. <https://doi.org/10.1016/j.atmosenv.2012.04.049>.
- Henze, D.K., Seinfeld, J.H., Ng, N.L., et al., 2008. Global modeling of secondary organic aerosol formation from aromatic hydrocarbons: high- vs. low-yield pathways. *Atmos. Chem. Phys.* 8, 2405–2420. <https://doi.org/10.5194/acp-8-2405-2008>.
- Huang, R.J., Zhang, Y., Bozzetti, C., et al., 2014. High secondary aerosol contribution to particulate pollution during haze events in China. *Nature* 514 (7521), 218–222. <https://doi.org/10.1038/nature13774>.
- IPCC, 2013. *Impacts, Adaptation and Vulnerability: Working Group II Contribution to the Intergovernmental Panel on Climate Change: Fifth Assessment Report (AR5): Summary for Policymakers*, Intergovernmental Panel on Climate Change. Working Group Impacts.
- Jordan, C., Fitz, E., Hagan, T., et al., 2009. Long-term study of VOCs measured with PTR-MS at a rural site in New Hampshire with urban influences. *Atmos. Chem. Phys.* 9 (14), 4677–4697. <https://doi.org/10.5194/acp-9-4677-2009>.
- Kaltonoudis, C., Kostenidou, E., Florou, K., et al., 2016. Temporal variability and sources of VOCs in urban areas of the eastern Mediterranean. *Atmos. Chem. Phys.* 16, 14825–14842. <https://doi.org/10.5194/acp-16-14825-2016>.
- Karl, T., Jobson, T., Kuster, W.C., et al., 2003. Use of proton-transfer-reaction mass spectrometry to characterize volatile organic compound sources at the La Porte super site during the Texas air quality study 2000. *J. Geophys. Res. Atmos.* 108, 4508. <https://doi.org/10.1029/2002jd003333>.
- Kim, E., Brown, S.G., Hafner, H.R., et al., 2005. Characterization of non-methane volatile organic compounds sources in Houston during 2001 using positive matrix factorization. *Atmos. Environ.* 39, 5934–5946. <https://doi.org/10.1016/j.atmosenv.2005.06.045>.
- Kim, K.H., Hong, Y.J., Pal, R., et al., 2008. Investigation of carbonyl compounds in air from various industrial emission sources. *Chemosphere* 70, 807–820. <https://doi.org/10.1016/j.chemosphere.2007.07.025>.
- Klimont, Z., Streets, D.G., Gupta, S., et al., 2002. Anthropogenic emissions of non-methane volatile organic compounds in China. *Atmos. Environ.* 36, 1309e1322. [https://doi.org/10.1016/S1352-2310\(01\)00529-5](https://doi.org/10.1016/S1352-2310(01)00529-5).
- Kristensson, A., Johansson, C., Westerholm, R., et al., 2004. Real-world traffic emission factors of gases and particles measured in a road tunnel in Stockholm, Sweden. *Atmos. Environ.* 38, 657–673. <https://doi.org/10.1016/j.atmosenv.2003.10.030>.
- Lewis, A.C., Carslaw, N., Marriott, P.J., et al., 2000. A large pool of ozone-forming carbon compounds in urban atmosphere. *Nature* 405 (6788), 778–781. <https://doi.org/10.1038/35015540>.
- Li, H.Y., He, Q.S., Song, Q., et al., 2017. Diagnosing Tibetan pollutant sources via volatile organic compound observations. *Atmos. Environ.* 166, 244e254. <https://doi.org/10.1016/j.atmosenv.2017.07.031>.
- Li, J., Wu, R.R., Li, Y.Q., et al., 2016. Effects of rigorous emission controls on reducing ambient volatile organic compounds in Beijing, China. *Sci. Total Environ.* 557–558, 531–541. <https://doi.org/10.1016/j.scitotenv.2016.03.140>.
- Li, J., Zhai, C., Yu, J., et al., 2018. Spatiotemporal variations of ambient volatile organic compounds and their sources in Chongqing, a mountainous megacity in China. *Sci. Total Environ.* 627, 1442–1452. <https://doi.org/10.1016/j.scitotenv.2018.02.010>.
- Li, L., Chen, Y., Zeng, L., et al., 2014. Biomass burning contribution to ambient volatile organic compounds (VOCs) in the Chengdu-Chongqing region (CCR), China. *Atmos. Environ.* 99, 403e410.
- Li, L., Xie, S., Zeng, L., et al., 2015. Characteristics of volatile organic compounds and their role in ground-level ozone formation in the Beijing-Tianjin-Hebei region, China. *Atmos. Environ.* 113, 247–254. <https://doi.org/10.1016/j.atmosenv.2015.05.021>.
- Liu, B., Liang, D., Yang, J., et al., 2016. Characterization and source apportionment of volatile organic compounds based on 1-year of observational data in Tianjin, China. *Environ. Pollut.* 218, 757e769. <https://doi.org/10.1016/j.envpol.2016.07.072>.
- Liu, Y., Shao, M., Lu, S.H., et al., 2008a. Volatile organic compound (VOC) measurements in the Pearl River Delta (PRD) region, China. *Atmos. Chem. Phys.* 8, 1531–1545. <https://doi.org/10.5194/acp-8-1531-2008>.
- Liu, Y., Shao, M., Lu, S., et al., 2008b. Source apportionment of ambient volatile organic compounds in the Pearl River Delta, China: part II. *Atmos. Environ.* 42, 6261e6274.
- Marc, M., Namiesnik, J., Zabiegała, B., 2014. BTEX concentration levels in urban air in the area of the Tri-city agglomeration (Gdansk, Gdynia, Sopot), Poland. *Air Qual. Atmos. Health* 7 (4), 489e504. <https://doi.org/10.1007/s11869-014-0247-x>.
- Millet, D.B., Jacob, D.J., Boersma, K.F., et al., 2008. Spatial distribution of isoprene emissions from North America derived from formaldehyde column measurements by the OMI satellite sensor. *J. Geophys. Res. Atmos.* 113, D02307. <https://doi.org/10.1029/2007JD008950>.
- Millet, D.B., Guenther, A., Siegel, D.A., et al., 2010. Global atmospheric budget of acetaldehyde: 3-D model analysis and constraints from in-situ and satellite observations. *Atmos. Chem. Phys.* 10, 3405–3425. <https://doi.org/10.5194/acp-10-3405-2010>.
- Mo, Z., Shao, M., Lu, S., et al., 2017. Characterization of non-methane hydrocarbons and their sources in an industrialized coastal city, Yangtze River Delta, China. *Sci. Total Environ.* 593–594, 641–653. <https://doi.org/10.1016/j.scitotenv.2017.03.123>.
- Ng, N.L., Kroll, J.H., Chan, A.W.H., et al., 2007. Secondary organic aerosol formation from m-xylene, toluene, and benzene. *Atmos. Chem. Phys.* 7, 3909–3922. <https://doi.org/10.5194/acp-7-3909-2007>.
- Paatero, P., 1997. Least squares formulation of robust non-negative factor analysis. *Chemom. Intell. Lab. Syst.* 37 (1), 23–35. [https://doi.org/10.1016/S0169-7439\(96\)00044-5](https://doi.org/10.1016/S0169-7439(96)00044-5).
- Paatero, P., Tapper, U., 1994. Positive matrix factorization: a non-negative factor model with optimal utilization of error estimates of data values. *Environmetrics* 5 (2), 111–126. <https://doi.org/10.1002/env.3170050203>.
- Pan, X., Kanaya, Y., Tanimoto, H., et al., 2015. Examining the major contributors of ozone pollution in a rural area of the Yangtze River Delta region during harvest season. *Atmos. Chem. Phys.* 15, 6101–6111. <https://doi.org/10.5194/acp-15-6101-2015>.
- Rantala, P., Järvi, L., Taipale, R., et al., 2016. Anthropogenic and biogenic influence on VOC fluxes at an urban background site in Helsinki, Finland. *Atmos. Chem. Phys.* 16, 7981–8007. <https://doi.org/10.5194/acp-16-7981-2016>.

- Robert, S.B., Paul, S.M., Andrew, M.E., 2009. Proton-transfer reaction mass spectrometry. *Chem. Rev.* 109, 861–896. <https://doi.org/10.1021/cr800364q>.
- Roberts, J.M., Fehsenfeld, F.C., Liu, S.C., et al., 1984. Measurements of aromatic hydrocarbon ratios and NOx concentrations in the rural troposphere: observation of air mass photochemical aging and NOx removal. *Atmos. Environ.* 18, 2421–2432. [https://doi.org/10.1016/0004-6981\(84\)90012-X](https://doi.org/10.1016/0004-6981(84)90012-X).
- Roberts, J.M., Veres, P., Boer, T.C., et al., 2014. New insights into atmospheric sources and sinks of isocyanic acid, HNC(O), from recent urban and regional observations. *J. Geophys. Res.-Atmos.* 119, 1060–1072. <https://doi.org/10.1002/2013JD019931>.
- Sahu, L.K., Yadav, R., Pal, D., 2016. Source identification of VOCs at an urban site of western India: effect of marathon events and anthropogenic emissions. *J. Geophys. Res.* Atmos. 121, 2416–2433. <https://doi.org/10.1002/2015JD024454>.
- Sarkar, C., Sinha, V., Kumar, V., et al., 2016. Overview of VOC emissions and chemistry from PTR-TOF-MS measurements during the SusKat-ABC campaign: high acetaldehyde, isoprene and isocyanic acid in wintertime air of the Kathmandu Valley. *Atmos. Chem. Phys.* 16, 3979–4003. <https://doi.org/10.5194/acpd-15-25021-2015>.
- Sarkar, C., Sinha, V., Sinha, B., et al., 2017. Source apportionment of NMVOCs in the Kathmandu Valley during the SusKat-ABC international field campaign using positive matrix factorization. *Atmos. Chem. Phys.* 17, 8129–8156. <https://doi.org/10.5194/acp-2016-1139>.
- Seinfeld, J.H., Pandis, S.N., 1998. *Atmospheric Chemistry and Physics*. John Wiley & Sons, Inc, New York, USA, pp. 724–743.
- Shao, P., An, J., Xin, J., et al., 2016. Source apportionment of VOCs and the contribution to photochemical ozone formation during summer in the typical industrial area in the Yangtze River Delta, China. *Atmos. Res.* 176–177, 64–74. <https://doi.org/10.1016/j.atmosres.2016.02.015>.
- Sinha, V., Kumar, V., Sarkar, C., et al., 2014. Chemical composition of pre-monsoon air in the indo-Gangetic plain measured using a new air quality facility and PTR-MS: high surface ozone and strong influence of biomass burning. *Atmos. Chem. Phys.* 14, 5921–5941. <https://doi.org/10.5194/acp-14-5921-2014>.
- Stockwell, C.E., Veres, P.R., Williams, J., et al., 2015. Characterization of biomass burning emissions from cooking fires, peat, crop residue, and other fuels with high-resolution proton-transfer-reaction time-of-flight mass spectrometry. *Atmos. Chem. Phys.* 15, 845–865. <https://doi.org/10.5194/acp-15-845-2015>.
- Stojić, A., Stojić, S.S., Šoštarić, A., et al., 2015. Characterization of VOC sources in an urban area based on PTR-MS measurements and receptor modelling. *Environ. Sci. Pollut. Res.* 22 (17), 13137–13152. <https://doi.org/10.1007/s11356-015-4540-5>.
- Stone, E.A., Schauer, J.J., Pradhan, B.B., et al., 2010. Characterization of emissions from South Asian biofuels and application to source apportionment of carbonaceous aerosol in the Himalayas. *J. Geophys. Res.-Atmos.* 115, D06301. <https://doi.org/10.1029/2009jd011881>.
- Sun, J., Wu, F.K., Hu, B., et al., 2016. VOC characteristics, emissions and contributions to SOA formation during hazy episodes. *Atmos. Environ.* 141, 560e570. <https://doi.org/10.1016/j.atmosenv.2016.06.060>.
- Taipale, R., Ruuskanen, T.M., Rinne, J., et al., 2008. Technical note: quantitative long-term measurements of VOC concentrations by PTR-MS— measurement, calibration, and volume mixing ratio calculation methods. *Atmos. Chem. Phys.* 8 (22), 6681–6698. <https://doi.org/10.5194/acp-8-6681-2008>.
- Tang, X.Y., Li, J.L., Dong, Z.X., et al., 1989. Photochemical pollution in Lanzhou, China—a case study. *J. Environ. Sci.* 58 (1), 384–395.
- U.S. EPA, 2014. EPA Positive Matrix Factorization (PMF) 5.0 Fundamentals and User Guide. <http://www.epa.gov/heasd/research/pmf.html> (accessed in May 2015).
- U.S. EPA (U.S. Environmental Protection Agency), 1994. Locating and Estimating Documents, Office of Air Planning and Standards. U.S. Environmental Protection Agency, Research Triangle Park, North Carolina.
- Valach, A.C., Langford, B., Nemitz, E., et al., 2015. Seasonal and diurnal trends in concentrations and fluxes of volatile organic compounds in Central London. *Atmos. Chem. Phys.* 15, 7777–7796. <https://doi.org/10.5194/acp-15-7777-2015>.
- Wang, M., Shao, M., Lu, S.H., et al., 2013. Evidence of coal combustion contribution to ambient VOCs during winter in Beijing. *Chin. Chem. Lett.* 24 (9), 829e832. <https://doi.org/10.1016/j.ccllet.2013.05.029>.
- Wang, Y.N., Jia, C., Tao, J., et al., 2016. Chemical characterization and source apportionment of PM2.5 in a semi-arid and petrochemical industrialized city, Northwest China. *Sci. Total Environ.* 573, 1031–1040. <https://doi.org/10.1016/j.scitotenv.2016.08.179>.
- Wang, Y.Q., Zhang, X.Y., Draxler, R., 2009. TrajStat: GIS-based software that uses various trajectory statistical analysis methods to identify potential sources from long-term air pollution measurement data. *Environ. Model. Softw.* 24, 938e939.
- Warneke, C., McKeen, S.A., de Gouw, J.A., et al., 2007. Determination of urban volatile organic compound emission ratios and comparison with an emissions database. *J. Geophys. Res.* 112, D10S47. <https://doi.org/10.1029/2006JD007930>.
- Warneke, C., Roberts, J.M., Veres, P., et al., 2011. VOC identification and inter-comparison from laboratory biomass burning using PTR-MS and PIT-MS. *Int. J. Mass Spectrom.* 303, 6–14. <https://doi.org/10.1016/j.ijms.2010.12.002>.
- Watson, J.G., Chow, J.C., Fujita, E.M., 2001. Review of volatile organic compound source apportionment by chemical mass balance. *Atmos. Environ.* 35, 1567e1584. [https://doi.org/10.1016/s1352-2310\(00\)00461-1](https://doi.org/10.1016/s1352-2310(00)00461-1).
- White, M., Russo, R., Zhou, Y., et al., 2008. Volatile organic compounds in northern New England marine and continental environments during the ICARTT 2004 campaign. *J. Geophys. Res.* 113, D08S90. <https://doi.org/10.1029/2007JD009161>.
- WHO, 2016. [http://www.who.int/phe/health\\_topics/outdoorair/databases/en/](http://www.who.int/phe/health_topics/outdoorair/databases/en/).
- WHO Guidelines for Indoor Air Quality: Selected Pollutants, 2010. edited by: Theakston, F., World Health Organization: WHO Regional Office for Europe, Copenhagen, Denmark, 1–454.
- Yan, Y.L., Peng, L., Li, R.M. et al., 2017. Concentration, ozone formation potential and source analysis of volatile organic compounds (VOCs) in a thermal power station centralized area: a study in Shuozhou, China. *Environ. Pollut.* 223, 295e304. <https://doi.org/10.1016/j.envpol.2017.01.026>.
- Yoshino, A., Nakashima, Y., Miyazaki, K., et al., 2012. Air quality diagnosis from comprehensive observations of total OH reactivity and reactive trace species in urban Central Tokyo. *Atmos. Environ.* 49, 51e59. <https://doi.org/10.1016/j.atmosenv.2011.12.029>.
- Yuan, B., Shao, M., Lu, S., et al., 2010. Source profiles of volatile organic compounds associated with solvent use in Beijing, China. *Atmos. Environ.* 44, 1919–1926. <https://doi.org/10.1016/j.atmosenv.2010.02.014>.
- Yuan, B., Hu, W.W., Shao, M., et al., 2013. VOC emissions, evolutions and contributions to SOA formation at a receptor site in eastern China. *Atmos. Chem. Phys.* 13, 8815–8832. <https://doi.org/10.5194/acp-13-8815-2013>.
- Yuan, B., Koss, A.R., Warneke, C., et al., 2017. Proton-transfer-reaction mass spectrometry: applications in atmospheric sciences. *Chem. Rev.* 117 (21), 13187–13229. <https://doi.org/10.1021/acs.chemrev.7b00325>.
- Yuan, Z., Lau, A.K.H., Shao, M., et al., 2009. Source analysis of volatile organic compounds by positive matrix factorization in urban and rural environments in Beijing. *J. Geophys. Res.* 114 (16), D00G15. <https://doi.org/10.1029/2008JD011190>.
- Zhang, Y., Wang, X., Zhang, Z., et al., 2015. Sources of C2–C4 alkenes, the most important ozone nonmethane hydrocarbon precursors in the Pearl River Delta region. *Sci. Total Environ.* 502, 236–245. <https://doi.org/10.1016/j.scitotenv.2014.09.024>.
- Zheng, H., Kong, S.F., Xing, X.L., et al., 2018. Monitoring of volatile organic compounds (VOCs) from an oil and gas station in Northwest China for 1 year. *Atmos. Chem. Phys.* 18, 4567–4595. <https://doi.org/10.5194/acp-18-4567-2018>.
- Zhou, X., Zhang, T., Li, Z., et al., 2018. Particulate and gaseous pollutants in a petrochemical industrialized valley city, Western China during 2013–2016. *Environ. Sci. Pollut. Res.* 25 (15), 174–190. <https://doi.org/10.1007/s11356-018-1670-6>.
- Zhu, H., Wang, H., Jing, S., et al., 2018. Characteristics and sources of atmospheric volatile organic compounds (VOCs) along the mid-lower Yangtze River in China. *Atmos. Environ.* 190, 232–240. <https://doi.org/10.1016/j.atmosenv.2018.07.026>.
- Zou, Y., Deng, X.J., Zhu, D., et al., 2015. Characteristics of 1 year of observational data of VOCs, NOx and O3 at a suburban site in Guangzhou, China. *Atmos. Chem. Phys.* 15, 6625–6636. <https://doi.org/10.5194/acp-15-6625-2015>.